Multiscale analysis in image processing

Scale invariance in data processing

Barbara Pascal[†] and Nelly Pustelnik[‡]

bpascal-fr.github.io/talks

June 2025

[†] Nantes Université, École Centrale Nantes, CNRS, LS2N, F-44000 Nantes, France

[‡] CNRS, ENSL, Laboratoire de physique, F-69342 Lyon, France

Self-similarity in signals and images

Self-similar fields

$\mathsf{F} : \mathbb{R}^d \to \mathbb{R}$ a random field is **self-similar** if there exists $H \in (0,1)$ s.t.

$$(\forall c > 0) \quad \{\mathsf{F}(c\underline{x}); \underline{x} \in \mathbb{R}^N\} \overset{\text{(d)}}{=} c^H \{\mathsf{F}(\underline{x}); \underline{x} \in \mathbb{R}^d\}$$

with $\overset{\text{(d)}}{=}$ equality in distribution $\Longrightarrow H$: **fractal** index

Self-similar fields

$\mathsf{F} : \mathbb{R}^d \to \mathbb{R}$ a random field is **self-similar** if there exists $H \in (0,1)$ s.t.

$$(\forall c > 0) \quad \{\mathsf{F}(c\underline{x}); \underline{x} \in \mathbb{R}^N\} \overset{\text{(d)}}{=} c^H \{\mathsf{F}(\underline{x}); \underline{x} \in \mathbb{R}^d\}$$

with $\overset{\text{(d)}}{=}$ equality in distribution $\Longrightarrow H$: **fractal** index

Time series $\{\mathsf{F}(t),\, t \in \mathbb{R}\}$

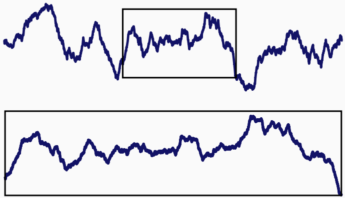

Images $\mathsf{F} : \Omega \subset \mathbb{R}^2 \to \mathbb{R}$

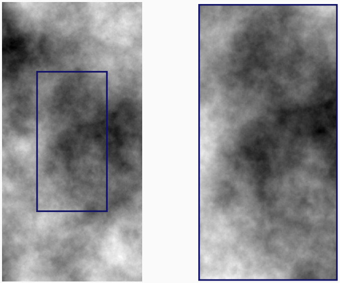

PREMIER COLLOQUE IMAGE
Traitement, Synthèse, Technologie et Applications

BIARRITZ — Mai 1984 —

LES FRACTALES: OBJETS MATHÉMATIQUES, MODÈLES PHYSIQUES ET CRÉATIONS ARTISTIQUES

Benoit B. MANDELBROT

IBM Thomas J. Watson Research Center, Yorktown Heights, NY, 10598, USA

RESUME

La géométrie fractale de la nature fut conçue et développée par l'auteur de ce travail et présentée pour la

SUMMARY

The fractal geometry of nature was conceived and developed by the author, beginning in 1975. It started with

"La géométrie fractal de la nature fut conçue et développée par l'auteur de ce travail et présentée pour la première fois en 1975. Ses sources se trouvent dans deux découvertes inattendues, aux multiples effets cumulatifs. Les fractales ont contribué à redonné (sic) *aux mathématiques et à la physique un côté visuel et presque sensuel, et elles ont posé des questions nouvelles concernant l'esthétique et de nombreux problèmes d'informatique et d'infographie."*

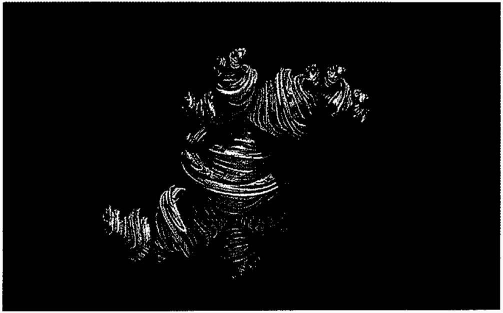

Figure 4 Dragon fractal quaternionique, réalisé par V. Alan Norton. Copyright 1983 by V. Alan Norton.

[B. B. Mandelbrot, 1983, "The fractal geometry of nature.", *W. H. Freeman and Co.*; B. B. Mandelbrot, 1984, *Colloque Images*]

Fractal objects in signal and image processing

- Physics: turbulent flows, geophysics [M. Nelkin, 1989, *J. Stat. Phys.*; B. Dubrulle, et al., 2022, *Philos. Trans. R. Soc. A.*]
- Financial forecasting [R.T. Baillie, ,1996, *J. Econom.*]
- Geography: relief representation, population in cities [L. Lucido, et al., 1998, *Int. J. Syst. Sci.*; J. Lengyel et al., 2025, *Sci. Rep.*]
- Cardiac activity mother-fetus [M. Doret et al., 2015, *PloS One.*]
- Computer networks analysis, Internet traffic
  [J. Beran et al., 1995, *IEEE Trans. Commun.*;
  P. Abry, et al., 1998, *IEEE Trans. Inf. Theory*;
  R. Fontugne, et al., 2017, *IEEE/ACM Trans. Network.*]
- Infographics/computer graphics
  [J. L., Encarnação et al., 2012, *Springer Science & Business Media.*]

Isotropic texture segmentation

Intuition and examples of texture

Texture: periodically and/or stochastically repeated pattern.

Intuition and examples of texture

Texture: periodically and/or stochastically repeated pattern.

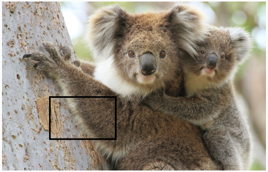

Intuition and examples of texture

Texture: periodically and/or stochastically repeated pattern.

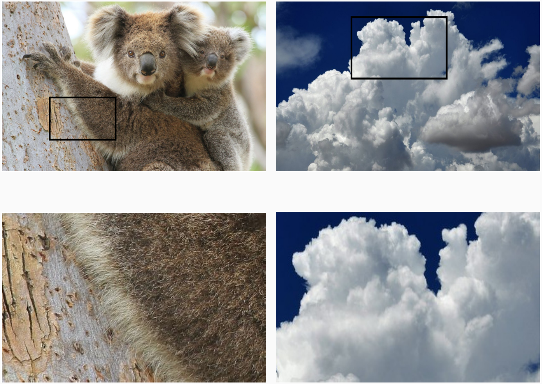

Intuition and examples of texture

Texture: periodically and/or stochastically repeated pattern.

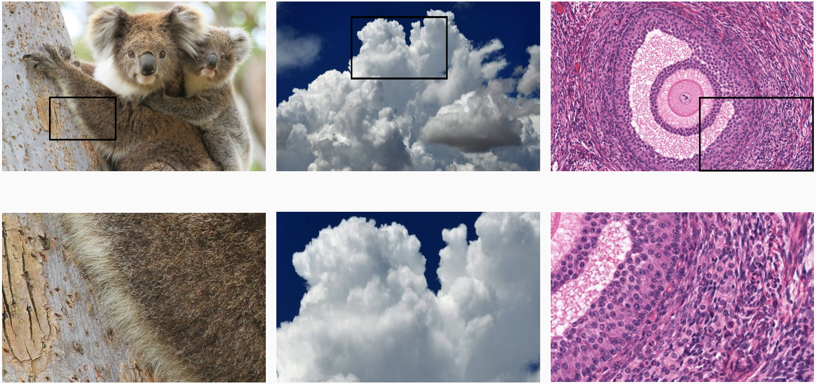

Intuition and examples of texture

Texture: periodically and/or stochastically repeated pattern.

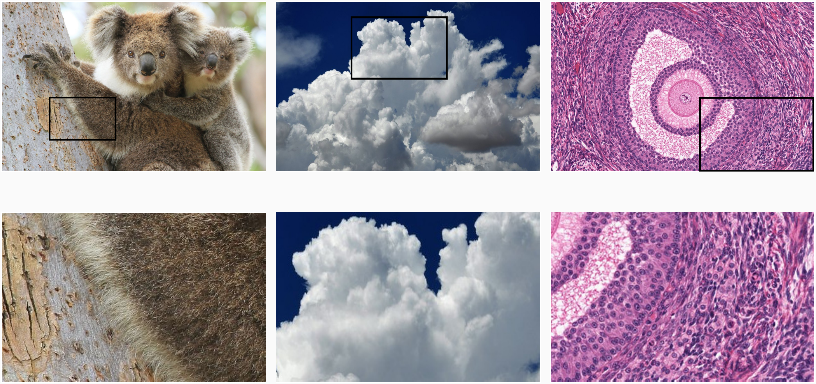

Crucial to describe and to process **real-world** images

Textured image segmentation

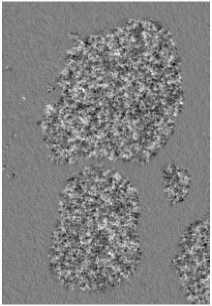

Textured image segmentation

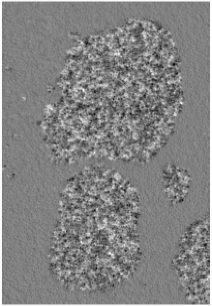

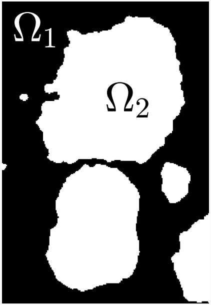

Goal: obtain a partition of the image into L homogeneous textures

$$\Omega = \Omega_1 \bigsqcup \ldots \bigsqcup \Omega_L$$

Textured image segmentation

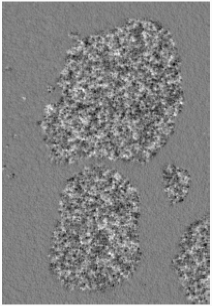

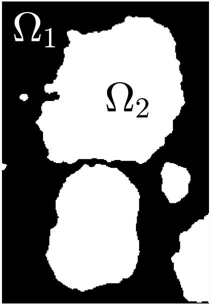

Goal: obtain a partition of the image into L **homogeneous textures**

$$\Omega = \Omega_1 \bigsqcup \ldots \bigsqcup \Omega_L$$

Features describing fractal textures

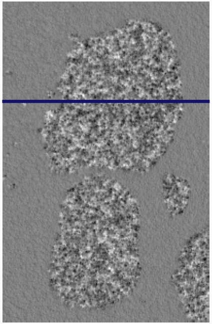

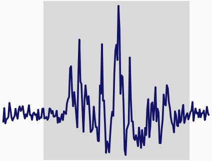

Features describing fractal textures

Fractals attributes

- variance σ^2 *amplitude of variations*

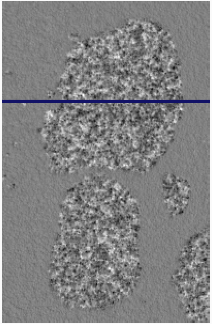

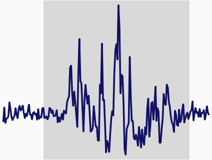

Features describing fractal textures

Fractals attributes

- variance σ^2 *amplitude of variations*
- local regularity h *scale invariance*

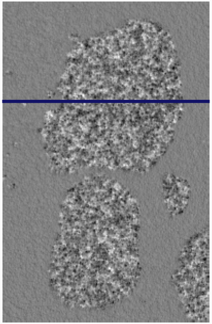

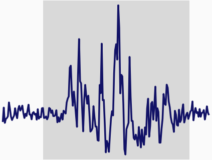

Features describing fractal textures

Fractals attributes

- variance σ^2 — *amplitude of variations*
- local regularity h — *scale invariance*

$$|f(\underline{x}) - f(\underline{y})| \leq \sigma(\underline{x})|\underline{x} - \underline{y}|^{h(\underline{x})}$$

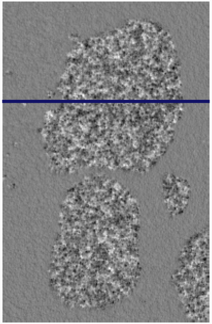

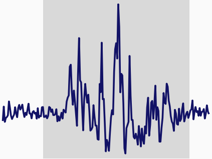

Features describing fractal textures

Fractals attributes

- variance σ^2 *amplitude of variations*
- local regularity h *scale invariance*

$$|f(\underline{x}) - f(\underline{y})| \leq \sigma(\underline{x})|\underline{x} - \underline{y}|^{h(\underline{x})}$$

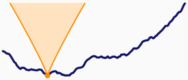

$h(\underline{x}) \equiv H_1 = 0.9$

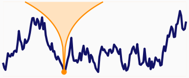

$h(\underline{x}) \equiv H_2 = 0.3$

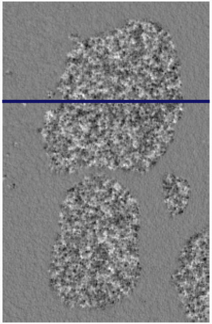

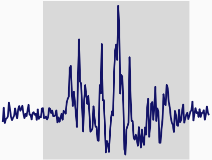

Features describing fractal textures

Fractals attributes

- <u>variance σ^2</u> *amplitude of variations*
- <u>local regularity h</u> *scale invariance*

$$|f(\underline{x}) - f(\underline{y})| \leq \sigma(\underline{x})|\underline{x} - \underline{y}|^{h(\underline{x})}$$

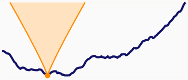

$h(\underline{x}) \equiv H_1 = 0.9$

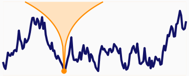

$h(\underline{x}) \equiv H_2 = 0.3$

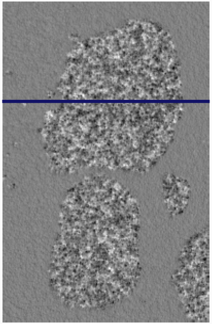

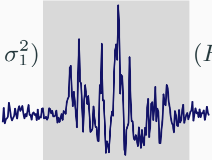

Segmentation

- h and σ^2 piecewise constant

Features describing fractal textures

Fractals attributes

- variance σ^2 *amplitude of variations*
- local regularity h *scale invariance*

$$|f(\underline{x}) - f(\underline{y})| \leq \sigma(\underline{x})|\underline{x} - \underline{y}|^{h(\underline{x})}$$

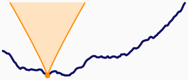

$h(\underline{x}) \equiv H_1 = 0.9$

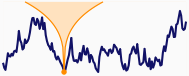

$h(\underline{x}) \equiv H_2 = 0.3$

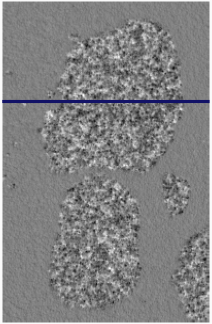

(H_2, σ_2^2)

(H_1, σ_1^2)

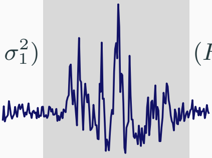

(H_1, σ_1^2)

Segmentation

- h and σ^2 piecewise constant
- region Ω_k characterized by (H_k, σ_k^2)

Self-similar Gaussian Fields: a few models

Let $H \in (0,1)$ be a so-called **Hurst index**; $\sigma^2 > 0$ a variance;
$\widetilde{\mathrm{W}}$ the Fourier transform of a Wiener measure.

Self-similar Gaussian Fields: a few models

Let $H \in (0,1)$ be a so-called **Hurst index**; $\sigma^2 > 0$ a variance;
$\widetilde{\mathrm{W}}$ the Fourier transform of a Wiener measure.

- **Fractional Brownian Field** $\mathrm{B}_H(\underline{x}) = \frac{\sigma}{\sqrt{\mathcal{C}_H}} \int_{\mathbb{R}^2} \frac{\mathrm{e}^{-\mathrm{i}\langle \underline{x}, \underline{\xi} \rangle} - 1}{\|\underline{\xi}\|^{H+1}} \widetilde{\mathrm{W}}(\mathrm{d}\underline{\xi})$

[B. B. Mandelbrot & J. W. Van Ness, 1968, *SIAM Rev.*]

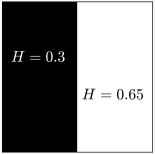

mask

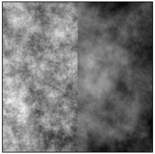
fBf B_H

Self-similar Gaussian Fields: a few models

Let $H \in (0,1)$ be a so-called **Hurst index**; $\sigma^2 > 0$ a variance;
$\widetilde{\mathsf{W}}$ the Fourier transform of a Wiener measure.

- **Fractional Brownian Field** $\quad \mathsf{B}_H(\underline{x}) = \dfrac{\sigma}{\sqrt{\mathcal{C}_H}} \displaystyle\int_{\mathbb{R}^2} \frac{\mathrm{e}^{-\mathrm{i}\langle \underline{x}, \underline{\xi} \rangle} - 1}{\|\underline{\xi}\|^{H+1}} \widetilde{\mathsf{W}}(\mathrm{d}\underline{\xi})$

  [B. B. Mandelbrot & J. W. Van Ness, 1968, *SIAM Rev.*]

- **Fractional Gaussian Field** [B. Pascal et al., 2021, *Appl. Comp. Harmon. Anal.*]

$$\mathsf{G}_H(\underline{x}) = \frac{1}{2} \underbrace{\left(\mathsf{B}_H(\underline{x} + \underline{\mathrm{e}}_1) - \mathsf{B}_H(\underline{x})\right)}_{\text{horizontal increment}} + \frac{1}{2} \underbrace{\left(\mathsf{B}_H(\underline{x} + \underline{\mathrm{e}}_2) - \mathsf{B}_H(\underline{x})\right)}_{\text{vertical increment}}$$

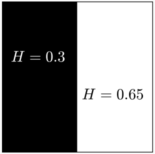

mask

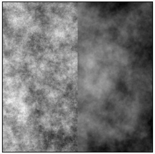
fBf B_H

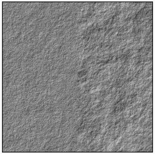
fGf G_H

Self-similar Gaussian Fields: a few models

Let $H \in (0,1)$ be a so-called **Hurst index**; $\sigma^2 > 0$ a variance;
$\widetilde{\mathrm{W}}$ the Fourier transform of a Wiener measure.

- **Fractional Brownian Field** $\quad \mathrm{B}_H(\underline{x}) = \dfrac{\sigma}{\sqrt{\mathcal{C}_H}} \displaystyle\int_{\mathbb{R}^2} \frac{\mathrm{e}^{-\mathrm{i}\langle \underline{x}, \underline{\xi} \rangle} - 1}{\|\underline{\xi}\|^{H+1}} \widetilde{\mathrm{W}}(\mathrm{d}\underline{\xi})$

  [B. B. Mandelbrot & J. W. Van Ness, 1968, *SIAM Rev.*]

- **Fractional Gaussian Field** [B. Pascal et al., 2021, *Appl. Comp. Harmon. Anal.*]

$$\mathrm{G}_H(\underline{x}) = \frac{1}{2}\underbrace{\left(\mathrm{B}_H(\underline{x} + \underline{\mathrm{e}}_1) - \mathrm{B}_H(\underline{x})\right)}_{\text{horizontal increment}} + \frac{1}{2}\underbrace{\left(\mathrm{B}_H(\underline{x} + \underline{\mathrm{e}}_2) - \mathrm{B}_H(\underline{x})\right)}_{\text{vertical increment}}$$

- **Filtered fBf** [B. Pascal et al., 2025, *IEEE Stat. Signal Process.*]

$\mathrm{C}_H(\underline{x}) = \langle \mathrm{B}_H, \mathrm{w}_{\underline{x}} \rangle$, w **isotropic** high-pass filter

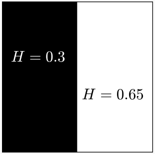

mask

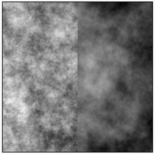
fBf B_H

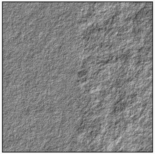
fGf G_H

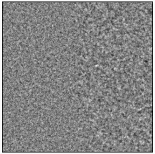
Filtered fBf

Synthetic fractal textures for performance assessment

How to choose a model to generate synthetic textures?

Synthetic fractal textures for performance assessment

How to choose a model to generate synthetic textures?

- visually resemble real textures: isotropic, stationary

Real

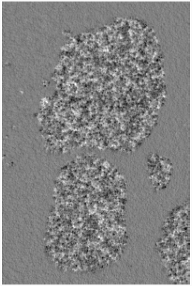

Synthetic fractal textures for performance assessment

How to choose a model to generate synthetic textures?

- visually resemble real textures: isotropic, stationary
- self-similar field characterized by (H, σ^2) such that $h(\underline{x}) \equiv H$

Real

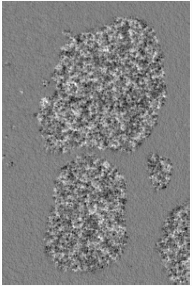

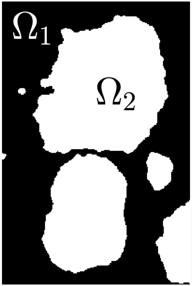

Synthetic fractal textures for performance assessment

How to choose a model to generate synthetic textures?

- visually resemble real textures: isotropic, stationary
- self-similar field characterized by (H, σ^2) such that $h(\underline{x}) \equiv H$
- easy to "patch": no artifact at the border

Real

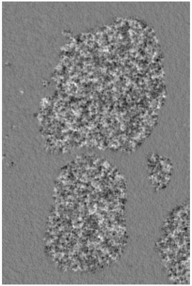

Mask

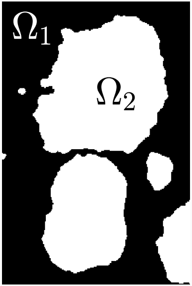

Synthetic fractal textures for performance assessment

How to choose a model to generate synthetic textures?

- visually resemble real textures: isotropic, stationary ✓
- self-similar field characterized by (H, σ^2) such that $h(\underline{x}) \equiv H$ ✓
- easy to "patch": no artifact at the border ✗

Real

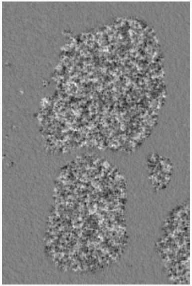

Mask

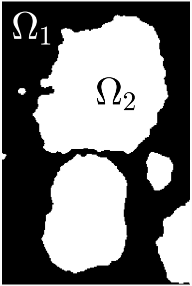

fBf

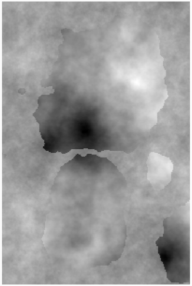

Synthetic fractal textures for performance assessment

How to choose a model to generate synthetic textures?

- visually resemble real textures: isotropic, stationary ✓
- self-similar field characterized by (H, σ^2) such that $h(\underline{x}) \equiv H$ ✓
- easy to "patch": no artifact at the border ✓

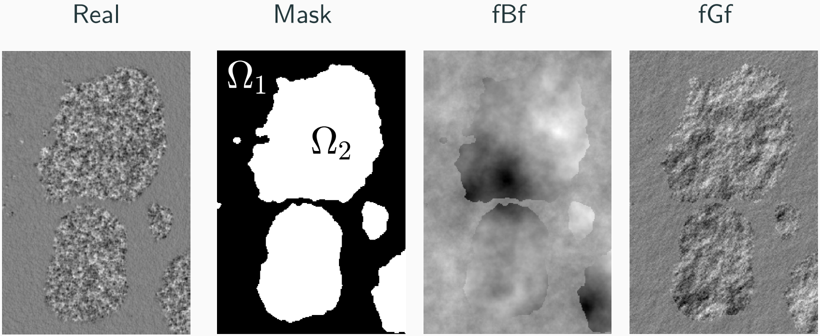

Multiscale analysis to probe local regularity

Field X $\in L^2(\mathbb{R}^2)$ and mother wavelet ψ with n_ψ **vanishing moments**

Proposition If the Hölder local regularity of F at $\underline{x}_0$ is $h(\underline{x}_0) \leq n_\psi$,

$$\exists A > 0, \quad |\mathcal{W}_f(\underline{x}, a)| \leq A a^{h(\underline{x}_0)+1} \left(1 + \left\| \frac{\underline{x}_0 - \underline{x}}{a} \right\|^{h(\underline{x}_0)} \right)$$

[S. Jaffard, 1991, *Publicacions Matemàtiques*]

Multiscale analysis to probe local regularity

Field $\mathsf{X} \in L^2(\mathbb{R}^2)$ and mother wavelet ψ with n_ψ **vanishing moments**

Proposition If the Hölder local regularity of F at $\underline{x}_0$ is $h(\underline{x}_0) \leq n_\psi$,

$$\exists A > 0, \quad |\mathcal{W}_f(\underline{x}, a)| \leq A a^{h(\underline{x}_0)+1} \left(1 + \left\| \frac{\underline{x}_0 - \underline{x}}{a} \right\|^{h(\underline{x}_0)}\right)$$

[S. Jaffard, 1991, *Publicacions Matemàtiques*]

Discrete wavelet coefficients $\zeta_{j,\underline{k}} = \langle \mathsf{X}, \psi_{j,\underline{k}} \rangle$ with ψ an L^1-normalized

$$|\zeta_{j,\underline{k}}^{(m)}| \underset{2^j \to 0}{\lesssim} \eta(\underline{n}) 2^{jh(\underline{n})}, \quad \text{for } \underline{n} = 2^j \underline{k}$$

with $\eta(\underline{n})$ some positive-valued function

Decimated wavelet leader coefficients

$$\widetilde{\mathcal{L}}_{j,\underline{k}}[\mathsf{X}] = \sup_{\substack{m=\{1,2,3\} \\ \lambda_{j',\underline{n}'} \subset 3\lambda_{j,\underline{n}}}} \left| 2^{j\gamma} \zeta^{(m)}_{j',\underline{k}'}[\mathsf{X}] \right|, \text{ with } \begin{cases} \lambda_{j,\underline{n}} = \left[\underline{k}2^j, (\underline{k}+1)2^j\right[\\ 3\lambda_{j,\underline{n}} = \bigcup_{\underline{p}\in\{-1,0,1\}^2} \lambda_{j,\underline{k}+\underline{p}}, \end{cases}$$

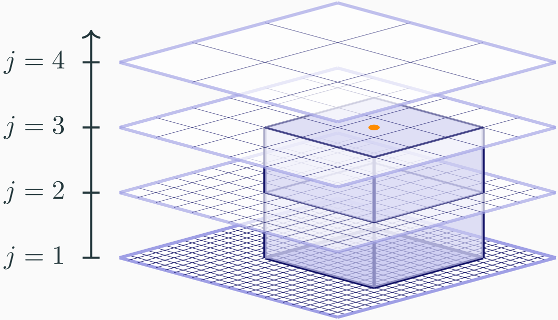

Wavelet p-Leader and Bootstrap based MultiFractal analysis (PLBMF)

irit.fr/∼Herwig.Wendt/software

Undecimated wavelet leader coefficients

$$\mathcal{L}_{j,\underline{n}}[\mathsf{X}] = \sup_{\substack{m=\{1,2,3\} \\ \lambda_{j',\underline{n}'} \subset 3\lambda_{j,\underline{n}}}} \left| 2^{j\gamma} \zeta^{(m)}_{j',\underline{n}'}[\mathsf{X}] \right|, \text{ with } \begin{cases} \lambda_{j,\underline{n}} = [\underline{n}, \underline{n} + 2^j [\\ 3\lambda_{j,\underline{n}} = \bigcup_{\underline{p} \in \{-2^j, 0, 2^j\}^2} \lambda_{j,\underline{n}+\underline{p}}, \end{cases}$$

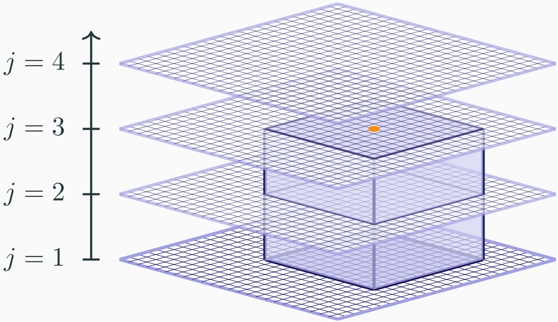

[S. Jaffard, 2004, *Proc. Symp. Pure Math.*;
H. Wendt et al., 2008, *IEEE T. Signal Proces.*]

Multiscale analysis

Textured image

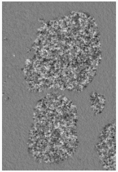

Multiscale analysis

Textured image

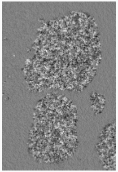

Local maximum of wavelet coefficients: $\mathcal{L}_{a,\cdot}$

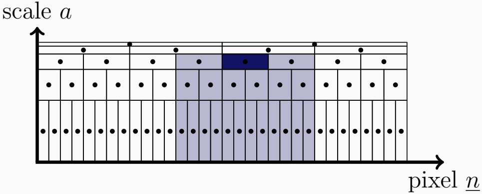

Multiscale analysis

Textured image

Local maximum of wavelet coefficients: $\mathcal{L}_{a,\cdot}$

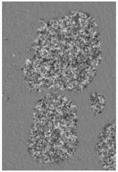

Scale

$a = 2^1$

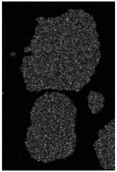

$a = 2^2$

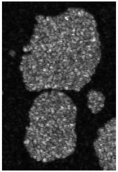

$\dots$

$a = 2^5$

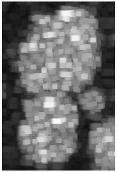

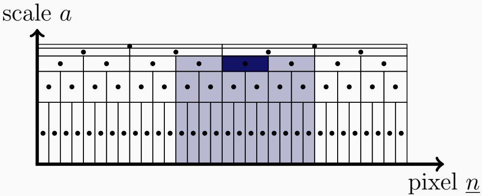

Multiscale analysis

Textured image

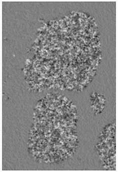

Local maximum of wavelet coefficients: $\mathcal{L}_{a,\cdot}$

Scale $a = 2^1$ $a = 2^2$ $a = 2^5$

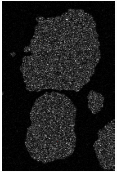

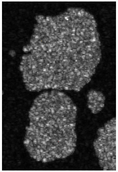

$\cdots$

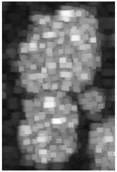

Proposition

$$\log\left(\mathcal{L}_{a,\cdot}\right) \underset{a \to 0}{\simeq} \log(a) \underbrace{\mathrm{h}}_{\text{regularity}} + \underbrace{\mathrm{v}}_{\substack{\propto \log(\boldsymbol{\sigma}^2) \\ \text{(variance)}}}$$

[S. Jaffard, 2004, *Proc. Symp. Pure Math.*;

H. Wendt et al., 2008, *IEEE T. Signal Proces.*]

Multiscale analysis

Textured image

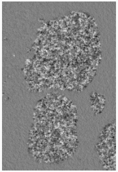

Local maximum of wavelet coefficients: $\mathcal{L}_{a,\cdot}$

Scale $a = 2^1$ $a = 2^2$ $\dots$ $a = 2^5$

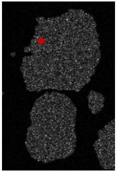

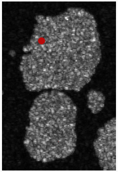

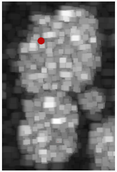

Proposition

$$\log\left(\mathcal{L}_{a,\cdot}\right) \underset{a\to 0}{\simeq} \log(a) \underbrace{\mathrm{h}}_{\text{regularity}} + \underbrace{\mathrm{v}}_{\substack{\propto \log(\boldsymbol{\sigma}^2) \\ \text{(variance)}}}$$

[S. Jaffard, 2004, *Proc. Symp. Pure Math.*;

H. Wendt et al., 2008, *IEEE T. Signal Proces.*]

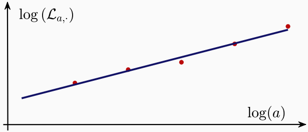

Multiscale analysis

Textured image

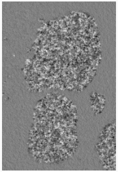

Local maximum of wavelet coefficients: $\mathcal{L}_{a,\cdot}$

Scale

$a = 2^1$

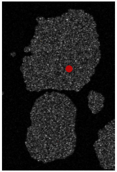

$a = 2^2$

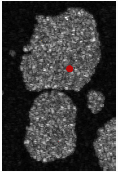

$\dots$

$a = 2^5$

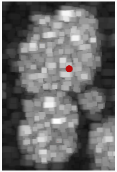

Proposition

$$\log\left(\mathcal{L}_{a,\cdot}\right) \underset{a\to 0}{\simeq} \log(a) \underbrace{\mathrm{h}}_{\text{regularity}} + \underbrace{\mathrm{v}}_{\substack{\propto \log(\boldsymbol{\sigma}^2) \\ \text{(variance)}}}$$

[S. Jaffard, 2004, *Proc. Symp. Pure Math.*;

H. Wendt et al., 2008, *IEEE T. Signal Proces.*]

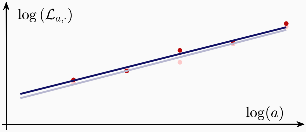

Multiscale analysis

Textured image

Local maximum of wavelet coefficients: $\mathcal{L}_{a,\cdot}$

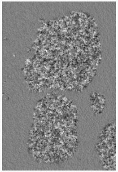

Scale $a = 2^1$ $a = 2^2$ $\cdots$ $a = 2^5$

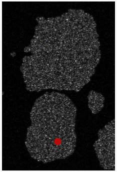

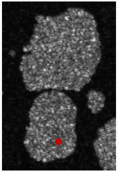

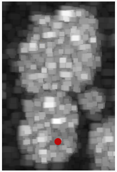

Proposition

$$\log\left(\mathcal{L}_{a,\cdot}\right) \underset{a \to 0}{\simeq} \log(a) \underbrace{\mathrm{h}}_{\text{regularity}} + \underbrace{\mathrm{v}}_{\substack{\propto \log(\boldsymbol{\sigma}^2) \\ \text{(variance)}}}$$

[S. Jaffard, 2004, *Proc. Symp. Pure Math.*;

H. Wendt et al., 2008, *IEEE T. Signal Proces.*]

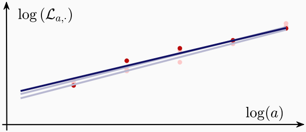

Multiscale analysis

Textured image

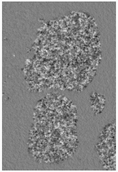

Local maximum of wavelet coefficients: $\mathcal{L}_{a,\cdot}$

Scale $a = 2^1$ $a = 2^2$ $\dots$ $a = 2^5$

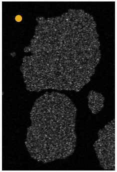

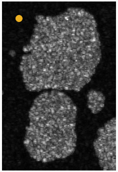

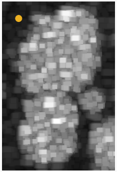

Proposition

$$\log\left(\mathcal{L}_{a,\cdot}\right) \underset{a\to 0}{\simeq} \log(a) \underset{\text{regularity}}{\mathrm{h}} + \underset{\substack{\propto \log(\boldsymbol{\sigma}^2)\\ \text{(variance)}}}{\mathrm{v}}$$

[S. Jaffard, 2004, *Proc. Symp. Pure Math.*;

H. Wendt et al., 2008, *IEEE T. Signal Proces.*]

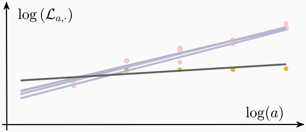

Multiscale analysis

Textured image

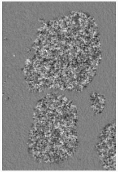

Local maximum of wavelet coefficients: $\mathcal{L}_{a,\cdot}$

Scale $a = 2^1$ $a = 2^2$ $\cdots$ $a = 2^5$

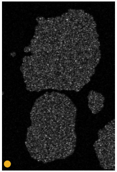

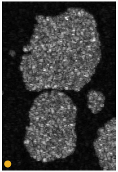

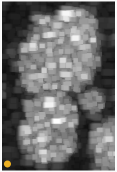

Proposition

$$\log\left(\mathcal{L}_{a,\cdot}\right) \underset{a\to 0}{\simeq} \log(a) \underbrace{\mathrm{h}}_{\text{regularity}} + \underbrace{\mathrm{v}}_{\substack{\propto\log(\boldsymbol{\sigma}^2)\\ \text{(variance)}}}$$

[S. Jaffard, 2004, *Proc. Symp. Pure Math.*;

H. Wendt et al., 2008, *IEEE T. Signal Proces.*]

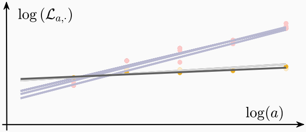

Multiscale analysis

Textured image

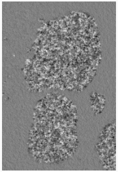

Local maximum of wavelet coefficients: $\mathcal{L}_{a,\cdot}$

Scale $a = 2^1$ $a = 2^2$ … $a = 2^5$

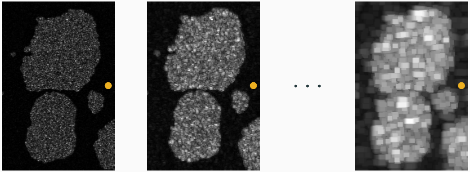

Proposition

$$\log\left(\mathcal{L}_{a,\cdot}\right) \underset{a\to 0}{\simeq} \log(a) \underset{\text{regularity}}{\mathrm{h}} + \underset{\substack{\propto \log(\boldsymbol{\sigma}^2) \\ \text{(variance)}}}{\mathrm{v}}$$

[S. Jaffard, 2004, *Proc. Symp. Pure Math.*;

H. Wendt et al., 2008, *IEEE T. Signal Proces.*]

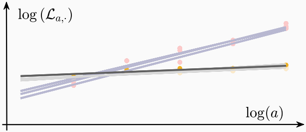

Direct punctual estimation

Linear regression $\log\left(\mathcal{L}_{a,\cdot}\right) \simeq \log(a) \underset{\text{regularity}}{\mathrm{h}} + \underset{\propto \log(\boldsymbol{\sigma}^2)}{\mathrm{v}}$

Textured image

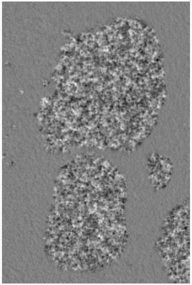

Direct punctual estimation

Linear regression $\log\left(\mathcal{L}_{a,\cdot}\right) \simeq \log(a) \underset{\text{regularity}}{\mathrm{h}} + \underset{\propto \log(\boldsymbol{\sigma}^2)}{\mathrm{v}}$

$$\left(\widehat{\mathrm{h}}^{\mathrm{LR}}, \widehat{\mathrm{v}}^{\mathrm{LR}}\right) = \underset{\mathrm{h},\mathrm{v}}{\operatorname{argmin}} \sum_{a=a_{\min}}^{a_{\max}} \left\|\log\left(\mathcal{L}_{a,\cdot}\right) - \log(a)\mathrm{h} - \mathrm{v}\right\|^2$$

Textured image

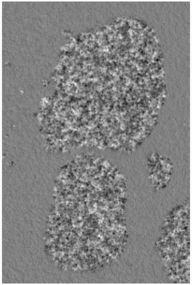

Direct punctual estimation

Linear regression $\log(\mathcal{L}_{a,\cdot}) \simeq \log(a) \underset{\text{regularity}}{\mathrm{h}} + \underset{\propto \log(\boldsymbol{\sigma}^2)}{\mathrm{v}}$

$$\left(\widehat{\mathrm{h}}^{\mathrm{LR}}, \widehat{\mathrm{v}}^{\mathrm{LR}}\right) = \underset{\mathrm{h},\mathrm{v}}{\operatorname{argmin}} \sum_{a=a_{\min}}^{a_{\max}} \left\|\log(\mathcal{L}_{a,\cdot}) - \log(a)\mathrm{h} - \mathrm{v}\right\|^2$$

Textured image

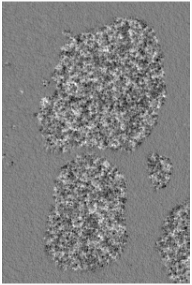

Local regularity $\widehat{\mathrm{h}}^{\mathrm{LR}}$

Local power $\widehat{\mathrm{v}}^{\mathrm{LR}}$

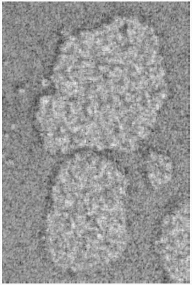

Direct punctual estimation

Linear regression $\underbrace{\mathbb{E}\log\left(\mathcal{L}_{a,\cdot}\right)}_{\text{expected value}} = \log(a)\underbrace{\bar{\mathrm{h}}}_{\text{regularity}} + \underbrace{\bar{\mathrm{v}}}_{\propto\log(\boldsymbol{\sigma}^2)}$

$$\left(\widehat{\mathrm{h}}^{\mathrm{LR}},\widehat{\mathrm{v}}^{\mathrm{LR}}\right) = \underset{\mathrm{h},\mathrm{v}}{\operatorname{argmin}} \sum_{a=a_{\min}}^{a_{\max}} \left\|\log\left(\mathcal{L}_{a,\cdot}\right) - \log(a)\mathrm{h} - \mathrm{v}\right\|^2$$

Textured image

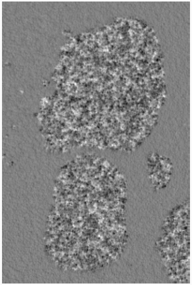

Local regularity $\widehat{\mathrm{h}}^{\mathrm{LR}}$

Local power $\widehat{\mathrm{v}}^{\mathrm{LR}}$

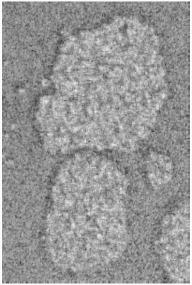

A posteriori regularization

Linear regression $\widehat{\mathrm{h}}^{\mathrm{LR}}$

A posteriori regularization

Finite differences $\mathrm{D}_1\mathrm{h}$ (horizontal), $\mathrm{D}_2\mathrm{h}$ (vertical) in each pixel

Linear regression $\widehat{\mathrm{h}}^{\mathrm{LR}}$

A posteriori regularization

Finite differences $\mathrm{Dx} = [\mathrm{D}_1\mathrm{h}, \mathrm{D}_2\mathrm{h}]$

Linear regression $\widehat{\mathrm{h}}^{\mathrm{LR}}$

A posteriori regularization

Finite differences $\mathrm{D}\mathrm{x} = [\mathrm{D}_1\mathrm{h}, \mathrm{D}_2\mathrm{h}]$

Filter smoothing (linear)

$$\underset{\mathrm{h}}{\operatorname{argmin}} \; \|\mathrm{h} - \widehat{\mathrm{h}}^{\mathrm{LR}}\|^2 + \theta\|\mathrm{D}\mathrm{h}\|_2^2$$
$$= \left(\mathrm{I} + \theta \mathrm{D}^\top \mathrm{D}\right)^{-1} \widehat{\mathrm{h}}^{\mathrm{LR}}$$

Linear regression $\widehat{\mathrm{h}}^{\mathrm{LR}}$

Smoothing

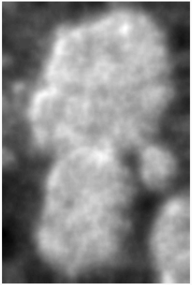

A posteriori regularization

Finite differences $\mathrm{Dx} = [\mathrm{D_1 h}, \mathrm{D_2 h}]$

Filter smoothing (linear)

$$\underset{\mathrm{h}}{\operatorname{argmin}} \ \|\mathrm{h} - \widehat{\mathrm{h}}^{\mathrm{LR}}\|^2 + \theta \|\mathrm{Dh}\|_2^2$$

$$= \left(\mathrm{I} + \theta \mathrm{D}^\top \mathrm{D}\right)^{-1} \widehat{\mathrm{h}}^{\mathrm{LR}}$$

ROF denoising (nonlinear)

$$\underset{\mathrm{h}}{\operatorname{argmin}} \ \|\mathrm{h} - \widehat{\mathrm{h}}^{\mathrm{LR}}\|^2 + \theta \|\mathrm{Dh}\|_{2,1}$$

[F. Abboud et al., 2017, *J. Math. Imaging Vis.*]

Linear regression $\widehat{\mathrm{h}}^{\mathrm{LR}}$ | Smoothing | ROF

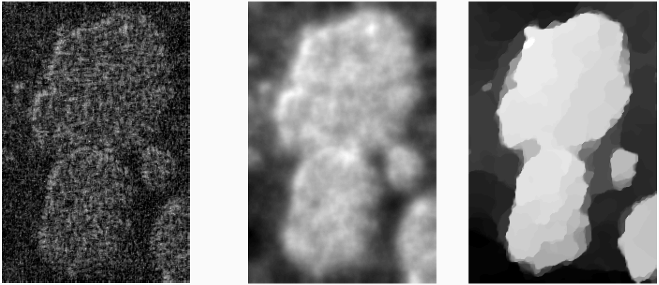

A posteriori regularization

Finite differences $\mathrm{D}\mathrm{x} = [\mathrm{D}_1\mathrm{h}, \mathrm{D}_2\mathrm{h}]$

Filter smoothing (linear)

$$\underset{\mathrm{h}}{\operatorname{argmin}} \; \|\mathrm{h} - \widehat{\mathrm{h}}^{\mathrm{LR}}\|^2 + \theta\|\mathrm{D}\mathrm{h}\|_2^2 = \left(\mathrm{I} + \theta \mathrm{D}^\top \mathrm{D}\right)^{-1} \widehat{\mathrm{h}}^{\mathrm{LR}}$$

ROF denoising (nonlinear)

$$\underset{\mathrm{h}}{\operatorname{argmin}} \; \|\mathrm{h} - \widehat{\mathrm{h}}^{\mathrm{LR}}\|^2 + \theta\|\mathrm{D}\mathrm{h}\|_{2,1}$$

[F. Abboud et al., 2017, *J. Math. Imaging Vis.*]

Linear regression $\widehat{\mathrm{h}}^{\mathrm{LR}}$ | Smoothing | ROF

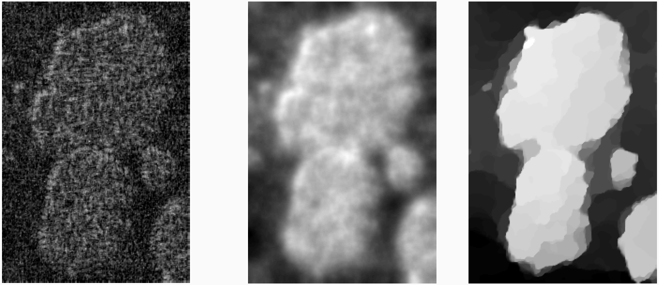

$\longrightarrow$ cumulative estimation variance and regularization bias

Functionals with either free or co-localized contours

$$\sum_a \underbrace{\|\log \mathcal{L}_{a,.} - \log(a)\mathrm{h} - \mathrm{v}\|^2}_{\substack{\textbf{Least-Squares} \\ \rightarrow \text{ fidelity to the log-linear model}}}$$

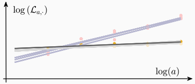

Functionals with either free or co-localized contours

$$\sum_a \underbrace{\|\log \mathcal{L}_{a,.} - \log(a)\mathrm{h} - \mathrm{v}\|^2}_{\textbf{Least-Squares}} + \theta_1 \underbrace{\mathcal{Q}(\mathrm{Dh}, \mathrm{Dv}; \theta_2)}_{\textbf{Total Variation}}$$

→ fidelity to the log-linear model

→ favors piecewise constancy

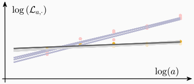

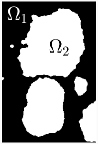

Functionals with either free or co-localized contours

$$\underset{\mathrm{h},\mathrm{v}}{\text{minimize}} \sum_a \underbrace{\|\log \mathcal{L}_{a,\cdot} - \log(a)\mathrm{h} - \mathrm{v}\|^2}_{\textbf{Least-Squares}} + \theta_1 \underbrace{\mathcal{Q}(\mathrm{Dh}, \mathrm{Dv}; \theta_2)}_{\textbf{Total Variation}}$$

$\rightarrow$ fidelity to the log-linear model

$\rightarrow$ favors piecewise constancy

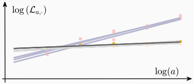

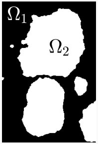

Functionals with either free or co-localized contours

$$\underset{\mathrm{h},\mathrm{v}}{\text{minimize}} \; \underbrace{\sum_a \|\log \mathcal{L}_{a,\cdot} - \log(a)\mathrm{h} - \mathrm{v}\|^2}_{\textbf{Least-Squares}} \; + \; \theta_1 \underbrace{\mathcal{Q}(\mathrm{Dh}, \mathrm{Dv}; \theta_2)}_{\textbf{Total Variation}}$$

$\rightarrow$ fidelity to the log-linear model

$\rightarrow$ favors piecewise constancy

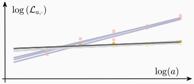

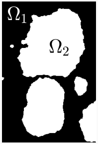

Finite differences $\mathrm{D}_1\mathrm{h}$ (horizontal), $\mathrm{D}_2\mathrm{h}$ (vertical) in each pixel

Functionals with either free or co-localized contours

$$\underset{\mathrm{h},\mathrm{v}}{\mathrm{minimize}} \sum_a \underbrace{\|\log \mathcal{L}_{a,.} - \log(a)\mathrm{h} - \mathrm{v}\|^2}_{\textbf{Least-Squares}} + \theta_1 \underbrace{\mathcal{Q}(\mathrm{Dh}, \mathrm{Dv}; \theta_2)}_{\textbf{Total Variation}}$$

$\rightarrow$ fidelity to the log-linear model

$\rightarrow$ favors piecewise constancy

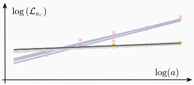

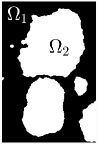

Finite differences $\mathrm{Dh} = [\mathrm{D}_1\mathrm{h}, \mathrm{D}_2\mathrm{h}]$

Free: h, v are **independently** piecewise constant

$$\mathcal{Q}_{\mathsf{F}}(\mathrm{Dh}, \mathrm{Dv}; \theta_2) = \theta_2 \|\mathrm{Dh}\|_{2,1} + \|\mathrm{Dv}\|_{2,1}$$

Functionals with either free or co-localized contours

$$\underset{\mathrm{h},\mathrm{v}}{\text{minimize}} \; \sum_a \underbrace{\|\log \mathcal{L}_{a,.} - \log(a)\mathrm{h} - \mathrm{v}\|^2}_{\textbf{Least-Squares}} \; + \; \theta_1 \underbrace{\mathcal{Q}(\mathrm{Dh}, \mathrm{Dv}; \theta_2)}_{\textbf{Total Variation}}$$

→ fidelity to the log-linear model

→ favors piecewise constancy

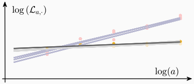

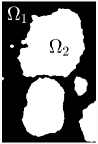

Finite differences $\mathrm{Dh} = [\mathrm{D}_1\mathrm{h}, \mathrm{D}_2\mathrm{h}]$

Free: h, v are **independently** piecewise constant

$$\mathcal{Q}_\mathsf{F}(\mathrm{Dh}, \mathrm{Dv}; \theta_2) = \theta_2\|\mathrm{Dh}\|_{2,1} + \|\mathrm{Dv}\|_{2,1}$$

Co-localized: h, v are **concomitantly** piecewise constant

$$\mathcal{Q}_\mathsf{C}(\mathrm{Dh}, \mathrm{Dv}; \theta_2) = \|[\theta_2\mathrm{Dh}, \mathrm{Dv}]\|_{2,1}$$

Functionals minimization

$$\underset{\mathrm{h},\mathrm{v}}{\text{minimize}} \quad \underbrace{\sum_a \|\log \mathcal{L}_{a,.} - \log(a)\mathrm{h} - \mathrm{v}\|^2}_{\textbf{Least-Squares}} \quad + \quad \theta_1 \underbrace{\mathcal{Q}(\mathrm{Dh}, \mathrm{Dv}; \theta_2)}_{\textbf{Total Variation}}$$

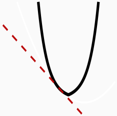

Functionals minimization

$$\underset{\mathrm{h},\mathrm{v}}{\text{minimize}} \; \sum_a \underbrace{\|\log \mathcal{L}_{a,.} - \log(a)\mathrm{h} - \mathrm{v}\|^2}_{\textbf{Least-Squares}} \;+\; \theta_1 \underbrace{\mathcal{Q}(\mathrm{Dh}, \mathrm{Dv}; \theta_2)}_{\textbf{Total Variation}}$$

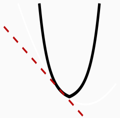

- gradient descent $\mathrm{x}^{[k+1]} = \mathrm{x}^{[k]} - \tau \nabla f(\mathrm{x}^{[k]})$ $\qquad \mathrm{x} = (\mathrm{h}, \mathrm{v})$

Functionals minimization

$$\underset{\mathrm{h},\mathrm{v}}{\text{minimize}} \quad \underbrace{\sum_a \|\log \mathcal{L}_{a,.} - \log(a)\mathrm{h} - \mathrm{v}\|^2}_{\textbf{Least-Squares}} \quad + \quad \theta_1 \underbrace{\mathcal{Q}(\mathrm{Dh}, \mathrm{Dv}; \theta_2)}_{\textbf{Total Variation}}$$

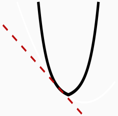

nonsmooth

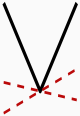

- gradient descent $\mathrm{x}^{[k+1]} = \mathrm{x}^{[k]} - \tau \nabla f(\mathrm{x}^{[k]})$ $\qquad \mathrm{x} = (\mathrm{h}, \mathrm{v})$
- implicit subgradient descent: proximal point algorithm

$$\mathrm{x}^{[k+1]} = \mathrm{x}^{[k]} - \tau \mathrm{u}^{[k]},\ \mathrm{u}^{[k]} \in \partial f(\mathrm{x}^{[k+1]}) \ \Leftrightarrow\ \mathrm{x}^{[k+1]} = \mathrm{prox}_{\tau f}(\mathrm{x}^{[k]})$$

Functionals minimization

$$\underset{\mathrm{h},\mathrm{v}}{\text{minimize}} \quad \sum_a \underbrace{\|\log \mathcal{L}_{a,\cdot} - \log(a)\mathrm{h} - \mathrm{v}\|^2}_{\textbf{Least-Squares}} \quad + \quad \theta_1 \underbrace{\mathcal{Q}(\mathrm{Dh}, \mathrm{Dv}; \theta_2)}_{\textbf{Total Variation}}$$

nonsmooth

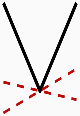

- gradient descent $\mathrm{x}^{[k+1]} = \mathrm{x}^{[k]} - \tau \nabla f(\mathrm{x}^{[k]})$ $\qquad \mathrm{x} = (\mathrm{h}, \mathrm{v})$
- implicit subgradient descent: proximal point algorithm

$$\mathrm{x}^{[k+1]} = \mathrm{x}^{[k]} - \tau \mathrm{u}^{[k]},\ \mathrm{u}^{[k]} \in \partial f(\mathrm{x}^{[k+1]}) \ \Leftrightarrow\ \mathrm{x}^{[k+1]} = \mathrm{prox}_{\tau f}(\mathrm{x}^{[k]})$$

- splitting proximal algorithm

$$\mathrm{u}^{[k+1]} = \mathrm{prox}_{\sigma(\theta\mathcal{Q})^*}\left(\mathrm{u}^{[k]} + \sigma \mathrm{D}\bar{\mathrm{x}}^{[k]}\right)$$

$$\mathrm{x}^{[k+1]} = \mathrm{prox}_{\tau\|\mathcal{L}-\mathrm{A}\cdot\|_2^2}\left(\mathrm{x}^{[k]} - \tau \mathrm{D}^\top \mathrm{u}^{[k+1]}\right), \quad \mathrm{A} : (\mathrm{h}, \mathrm{v}) \mapsto \{\log(a)\mathrm{h} + \mathrm{v}\}_a$$

$$\bar{\mathrm{x}}^{[k+1]} = 2\mathrm{x}^{[k+1]} - \mathrm{x}^{[k]}$$

[A. Chambolle et al., 2011, *J. Math. Imaging Vis.*]

Functionals minimization

$$\underset{\mathrm{h},\mathrm{v}}{\text{minimize}} \;\; \sum_a \underbrace{\|\log \mathcal{L}_{a,.} - \log(a)\mathrm{h} - \mathrm{v}\|^2}_{\textbf{Least-Squares}} \;\; + \;\; \theta_1 \underbrace{\mathcal{Q}(\mathrm{Dh}, \mathrm{Dv}; \theta_2)}_{\textbf{Total Variation}}$$

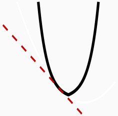

nonsmooth

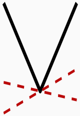

- gradient descent $\mathrm{x}^{[k+1]} = \mathrm{x}^{[k]} - \tau \nabla f(\mathrm{x}^{[k]})$ $\quad\quad \mathrm{x} = (\mathrm{h}, \mathrm{v})$
- implicit subgradient descent: proximal point algorithm

$$\mathrm{x}^{[k+1]} = \mathrm{x}^{[k]} - \tau \mathrm{u}^{[k]},\; \mathrm{u}^{[k]} \in \partial f(\mathrm{x}^{[k+1]}) \;\Leftrightarrow\; \mathrm{x}^{[k+1]} = \mathrm{prox}_{\tau f}(\mathrm{x}^{[k]})$$

- splitting proximal algorithm

$$\mathrm{u}^{[k+1]} = \mathrm{prox}_{\sigma(\theta\mathcal{Q})^*}\left(\mathrm{u}^{[k]} + \sigma \mathrm{D}\bar{\mathrm{x}}^{[k]}\right)$$

$$\mathrm{x}^{[k+1]} = \mathrm{prox}_{\tau\|\mathcal{L}-\mathrm{A}\cdot\|_2^2}\left(\mathrm{x}^{[k]} - \tau \mathrm{D}^\top \mathrm{u}^{[k+1]}\right), \quad \mathrm{A} : (\mathrm{h}, \mathrm{v}) \mapsto \{\log(a)\mathrm{h} + \mathrm{v}\}_a$$

$$\bar{\mathrm{x}}^{[k+1]} = 2\mathrm{x}^{[k+1]} - \mathrm{x}^{[k]}$$

[A. Chambolle et al., 2011, *J. Math. Imaging Vis.*]

Accelerated algorithm based on strong-convexity

$$\underset{\mathrm{h,v}}{\text{minimize}} \quad \underbrace{\sum_a \|\log \mathcal{L}_{a,.} - \log(a)\mathrm{h} - \mathrm{v}\|^2}_{\textbf{Least-Squares}} \quad + \quad \theta_1 \underbrace{\mathcal{Q}(\mathrm{Dh}, \mathrm{Dv}; \theta_2)}_{\textbf{Total Variation}}$$

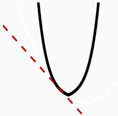

nonsmooth

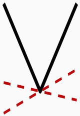

Primal-dual algorithm [A. Chambolle et al., 2011, *J. Math. Imaging Vis.*]

δ: duality gap, $\delta(\mathrm{x}^{[k]}, \mathrm{u}^{[k]}) \underset{n\to\infty}{\longrightarrow} 0$

Accelerated algorithm based on strong-convexity

$$\underset{\mathrm{h,v}}{\text{minimize}} \; \sum_a \underbrace{\|\log \mathcal{L}_{a,.} - \log(a)\mathrm{h} - \mathrm{v}\|^2}_{\textbf{Least-Squares}} \;+\; \theta_1 \underbrace{\mathcal{Q}(\mathrm{Dh}, \mathrm{Dv}; \theta_2)}_{\textbf{Total Variation}}$$

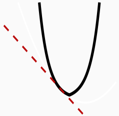

nonsmooth

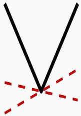

Primal-dual algorithm [A. Chambolle et al., 2011, *J. Math. Imaging Vis.*]

δ: duality gap, $\delta(\mathrm{x}^{[k]}, \mathrm{u}^{[k]}) \underset{n\to\infty}{\longrightarrow} 0$

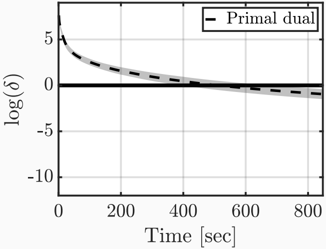

Convexity properties

$$\underset{\mathrm{h},\mathrm{v}}{\text{minimize}} \; \sum_a \underbrace{\|\log \mathcal{L}_{a,.} - \log(a)\mathrm{h} - \mathrm{v}\|^2}_{\textbf{Least-Squares}} \; + \; \theta_1 \underbrace{\mathcal{Q}(\mathrm{Dh}, \mathrm{Dv}; \theta_2)}_{\textbf{Total Variation}}$$

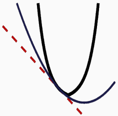

$\boldsymbol{\rho}$-strongly convex

nonsmooth

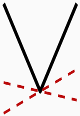

Convexity properties

$$\underset{\mathrm{h,v}}{\text{minimize}} \quad \underbrace{\sum_a \|\log \mathcal{L}_{a,.} - \log(a)\mathrm{h} - \mathrm{v}\|^2}_{\textbf{Least-Squares}} \quad + \quad \theta_1 \underbrace{\mathcal{Q}(\mathrm{Dh}, \mathrm{Dv}; \theta_2)}_{\textbf{Total Variation}}$$

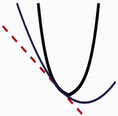

$\boldsymbol{\rho}$-strongly convex

nonsmooth

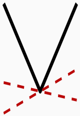

Strong-convexity

- f $\boldsymbol{\rho}$-strongly convex iff $f - \frac{\boldsymbol{\rho}}{2}\|\cdot\|^2$ convex

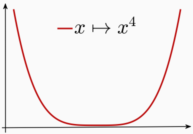

✓ strictly convex
✗ non strongly convex

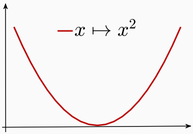

✓ strictly convex
✓ 1-strongly convex

Convexity properties

$$\underset{\mathrm{h},\mathrm{v}}{\text{minimize}} \quad \sum_a \underbrace{\|\log \mathcal{L}_{a,.} - \log(a)\mathrm{h} - \mathrm{v}\|^2}_{\textbf{Least-Squares}} \quad + \quad \theta_1 \underbrace{\mathcal{Q}(\mathrm{Dh}, \mathrm{Dv}; \theta_2)}_{\textbf{Total Variation}}$$

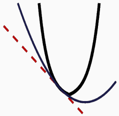

$\boldsymbol{\rho}$-strongly convex

nonsmooth

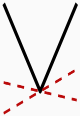

Strong-convexity

- f $\boldsymbol{\rho}$-strongly convex iff $f - \dfrac{\boldsymbol{\rho}}{2}\|\cdot\|^2$ convex
- f $\mathcal{C}^2$ with Hessian matrix $\mathrm{H}f \succeq 0 \implies \boldsymbol{\rho} = \min \mathrm{Sp}(\mathrm{H}f)$

Convexity properties

$$\underset{\mathrm{h},\mathrm{v}}{\text{minimize}} \ \underbrace{\sum_a \|\log \mathcal{L}_{a,.} - \log(a)\mathrm{h} - \mathrm{v}\|^2}_{\textbf{Least-Squares}} \quad + \quad \theta_1 \underbrace{\mathcal{Q}(\mathrm{Dh}, \mathrm{Dv}; \theta_2)}_{\textbf{Total Variation}}$$

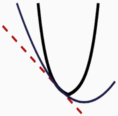

$\boldsymbol{\rho}$-strongly convex

nonsmooth

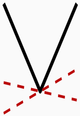

Strong-convexity

- f $\boldsymbol{\rho}$-strongly convex iff $f - \dfrac{\boldsymbol{\rho}}{2}\|\cdot\|^2$ convex
- f $\mathcal{C}^2$ with Hessian matrix $\mathrm{H}f \succeq 0 \implies \boldsymbol{\rho} = \min \mathrm{Sp}(\mathrm{H}f)$

Proposition $\sum_a \|\log \mathcal{L} - \log(a)\mathrm{h} - \mathrm{v}\|^2$ is $\boldsymbol{\rho}$-strongly convex.

$a_{\min} = 2^1$, $\quad a_{\max}$	2^2	2^3	2^4	2^5	2^6
$\boldsymbol{\rho} = \min \mathrm{Sp}\left(2\mathrm{A}^\top \mathrm{A}\right)$	0.29	**0.72**	1.20	1.69	2.20

[B. Pascal et al., 2021, *Appl. Comput. Harmon. Anal.*]

Accelerated algorithm based on strong-convexity

$$\underset{\mathrm{h},\mathrm{v}}{\text{minimize}} \; \underbrace{\sum_a \|\log \mathcal{L}_{a,\cdot} - \log(a)\mathrm{h} - \mathrm{v}\|^2}_{\textbf{Least-Squares}} \quad + \quad \theta_1 \underbrace{\mathcal{Q}(\mathrm{Dh}, \mathrm{Dv}; \theta_2)}_{\textbf{Total Variation}}$$

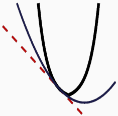

$\boldsymbol{\rho}$-strongly convex

nonsmooth

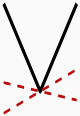

Accelerated Primal-dual algorithm [A. Chambolle et al., 2011, *J. Math. Imaging Vis.*]

for $k = 0, 1, \ldots$ $\qquad\qquad \mathrm{x} = (\mathrm{h}, \mathrm{v})$

$$\mathrm{u}^{[k+1]} = \mathrm{prox}_{\sigma_k (\theta \mathcal{Q})^*} \left(\mathrm{u}^{[k]} + \sigma_k \mathrm{D} \bar{\mathrm{x}}^{[k]} \right)$$

$$\mathrm{x}^{[k+1]} = \mathrm{prox}_{\tau_k \|\mathcal{L} - \mathrm{A}\cdot\|_2^2} \left(\mathrm{x}^{[k]} - \tau_k \mathrm{D}^\top \mathrm{u}^{[k+1]} \right)$$

$$\theta_k = \sqrt{1 + 2\boldsymbol{\rho}\tau_k}, \quad \tau_{n+1} = \tau_k / \theta_k, \quad \sigma_{n+1} = \theta_k \sigma_k$$

$$\bar{\mathrm{x}}^{[k+1]} = \mathrm{x}^{[k+1]} + \theta_k^{-1} \left(\mathrm{x}^{[k+1]} - \mathrm{x}^{[k]} \right)$$

Accelerated algorithm based on strong-convexity

$$\underset{\mathrm{h},\mathrm{v}}{\text{minimize}} \quad \underbrace{\sum_a \|\log \mathcal{L}_{a,.} - \log(a)\mathrm{h} - \mathrm{v}\|^2}_{\textbf{Least-Squares}} \quad + \quad \theta_1 \underbrace{\mathcal{Q}(\mathrm{Dh}, \mathrm{Dv}; \theta_2)}_{\textbf{Total Variation}}$$

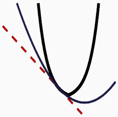

$\boldsymbol{\rho}$-strongly convex

nonsmooth

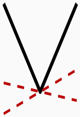

Accelerated Primal-dual algorithm [A. Chambolle et al., 2011, *J. Math. Imaging Vis.*]

δ: duality gap, $\delta(\mathrm{x}^{[k]}, \mathrm{u}^{[k]}) \underset{n\to\infty}{\longrightarrow} 0$

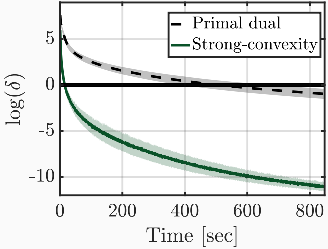

Segmentation *via* iterated thresholding

$$\underset{\mathrm{h},\mathrm{v}}{\text{minimize}} \sum_{a} \underbrace{\|\log \mathcal{L}_{a,.} - \log(a)\mathrm{h} - \mathrm{v}\|^2}_{\textbf{Least-Squares}} + \theta_1 \underbrace{\mathcal{Q}(\mathrm{Dh}, \mathrm{Dv}; \theta_2)}_{\textbf{Total Variation}}$$

Textured image

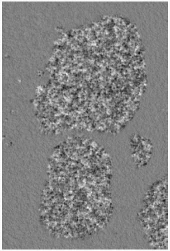

Lin. reg. $\widehat{\mathrm{h}}^{\mathrm{LR}}$

Segmentation *via* iterated thresholding

$$\underset{\mathrm{h},\mathrm{v}}{\text{minimize}} \ \sum_{a} \underbrace{\|\log \mathcal{L}_{a,.} - \log(a)\mathrm{h} - \mathrm{v}\|^2}_{\textbf{Least-Squares}} \ + \ \theta_1 \underbrace{\mathcal{Q}(\mathrm{Dh}, \mathrm{Dv}; \theta_2)}_{\textbf{Total Variation}}$$

Textured image

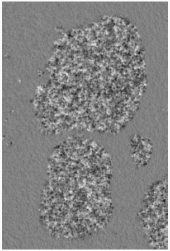

Lin. reg. $\widehat{\mathrm{h}}^{\mathrm{LR}}$

Co-localized contours $\widehat{\mathrm{h}}^{\mathrm{C}}$

[B. Pascal et al., 2021, *Appl. Comput. Harmon. Anal.*]

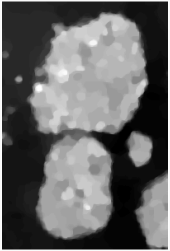

Threshold estimate† $T\widehat{\mathrm{h}}^{\mathrm{C}}$

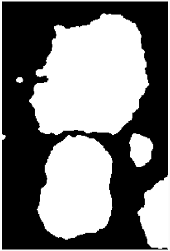

†Thresholding strategy from: [X. Cai et al., 2013, *EMMCVPR*]

State-of-the-art methods for texture segmentation

Threshold-ROF on $\widehat{\mathrm{h}}^{\mathrm{LR}}$

[C. Nafornita et al., 2014, *ICIP*; N. Pustelnik et al., 2016, *IEEE Trans. Comput. Imaging*]

$$\underset{\mathrm{h}}{\operatorname{argmin}} \; \|\mathrm{h} - \widehat{\mathrm{h}}^{\mathrm{LR}}\|^2 + \theta \|\mathrm{Dh}\|_{2,1}$$

Lin. reg. | ROF | Threshold

Only based on regularity h.

State-of-the-art methods for texture segmentation

Threshold-ROF on $\widehat{\mathrm{h}}^{\mathrm{LR}}$

[C. Nafornita et al., 2014, *ICIP*; N. Pustelnik et al., 2016, *IEEE Trans. Comput. Imaging*]

$$\underset{\mathrm{h}}{\operatorname{argmin}} \; \|\mathrm{h} - \widehat{\mathrm{h}}^{\mathrm{LR}}\|^2 + \theta \|\mathrm{Dh}\|_{2,1}$$

Lin. reg.	ROF	Threshold
		

Only based on regularity h.

Factorization based segmentation†

[J. Yuan, 2015, *IEEE Trans. Image Process.*]

(i) local histograms

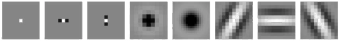

(ii) matrix factorization

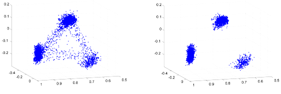

(a) (b)

Fig. 2. Scatterplot of features in subspace. (a) Scatterplot of features projected onto the 3-d subspace. (b) Scatterplot after removing features with high edgeness.

†https://sites.google.com/site/factorizationsegmentation/

Compared segmentation performance on synthetic textures

Piecewise monofractal texture synthesis

[B. Pascal et al., 2021, *Appl. Comput. Harmon. Anal.*]

mask: $\Omega = \Omega_1 \sqcup \Omega_2$,

attributes: $(H_\ell, \sigma_\ell^2)_{\ell=1,2}$

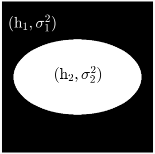

Compared segmentation performance on synthetic textures

Piecewise monofractal texture synthesis

[B. Pascal et al., 2021, *Appl. Comput. Harmon. Anal.*]

mask: $\Omega = \Omega_1 \sqcup \Omega_2$,

attributes: $(H_\ell, \sigma_\ell^2)_{\ell=1,2}$

Ex. $H_1 = 0.5, \quad \sigma_1^2 = 0.6$

$H_2 = 0.6, \quad \sigma_2^2 = 0.7$

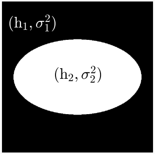

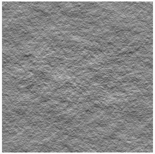

Compared segmentation performance on synthetic textures

Piecewise monofractal texture synthesis

[B. Pascal et al., 2021, *Appl. Comput. Harmon. Anal.*]

mask: $\Omega = \Omega_1 \sqcup \Omega_2$,

attributes: $(H_\ell, \sigma_\ell^2)_{\ell=1,2}$

Ex. $H_1 = 0.5, \quad \sigma_1^2 = 0.6$

$H_2 = 0.6, \quad \sigma_2^2 = 0.7$

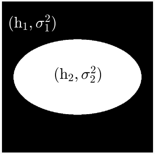

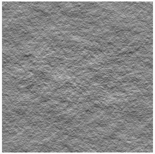

Averaged segmentation performances over 5 realizations

Yuan

$71.1 \pm 1.3\%$

T-ROF

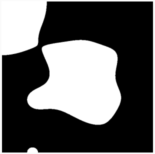

$78.5 \pm 1.1\%$

free contours

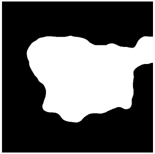

$90.2 \pm 1.9\%$

co-localized contours

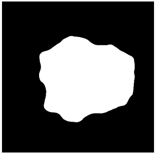

$91.1 \pm 1.5\%$

Multiphase flow through porous media

Laboratoire de Physique, ENS Lyon, V. Vidal, T. Busser, (M. Serres, IFPEN)

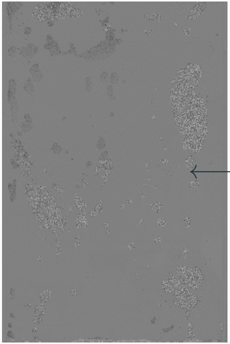

Solid foam

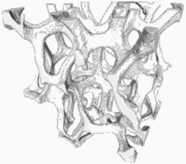

Multiphase flow through porous media

Laboratoire de Physique, ENS Lyon, V. Vidal, T. Busser, (M. Serres, IFPEN)

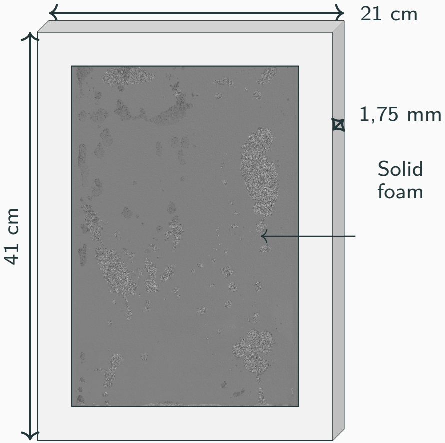

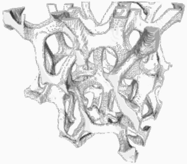

Multiphase flow through porous media

Laboratoire de Physique, ENS Lyon, V. Vidal, T. Busser, (M. Serres, IFPEN)

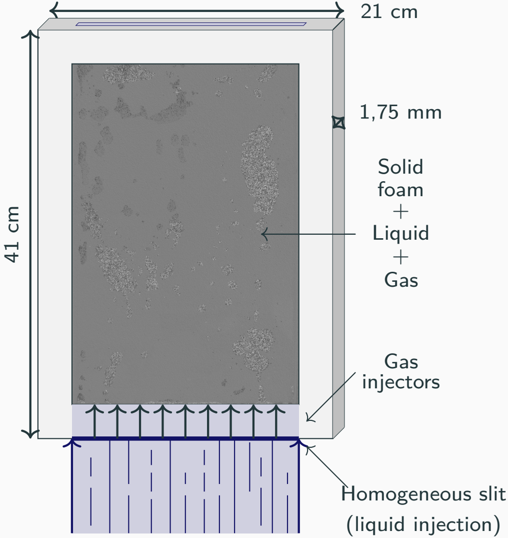

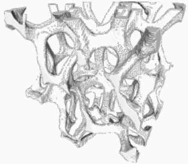

$\rightarrow$ 1600×1100 pixels
$\rightarrow$ video: ~ 1000 images
$\rightarrow$ phase diagram: ~ 10 flow rates

Low activity: $Q_{\mathrm{G}} = 300$mL/min - $Q_{\mathrm{L}} = 300$mL/min

Flow | Zooms | Yuan | T-ROF | Free contours | Co-localized contours

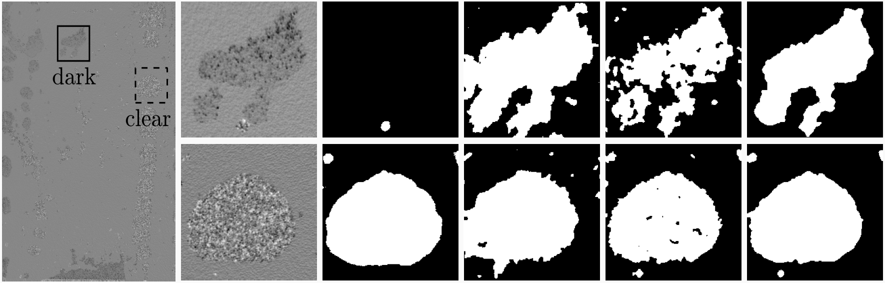

Low activity: $Q_{\mathrm{G}} = 300$mL/min - $Q_{\mathrm{L}} = 300$mL/min

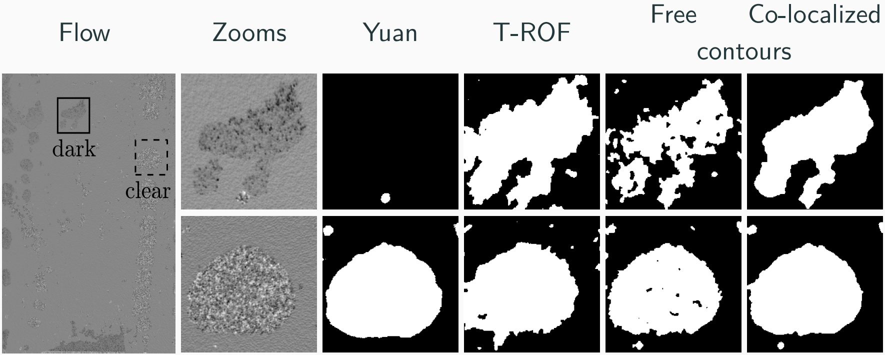

Liquid: $H_{\mathrm{L}} = 0.4$ $\quad \sigma^2_{\mathrm{dark}} = 10^{-2}$

Gas: $H_{\mathrm{G}} = 0.9$ $\left| \begin{array}{ll} \sigma^2_{\mathrm{dark}} = 10^{-2} & \text{(dark bubbles)} \\ \sigma^2_{\mathrm{clear}} = 10^{-1} & \text{(clear bubbles)} \end{array} \right.$

Transition: $Q_{\mathrm{G}} = 400$mL/min - $Q_{\mathrm{L}} = 700$mL/min

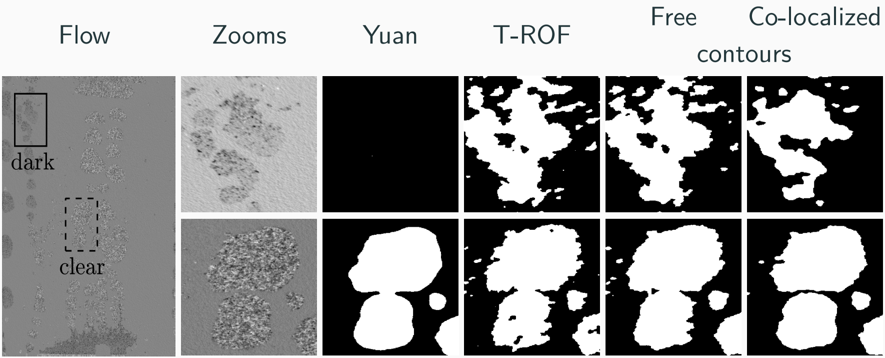

Liquid: $H_{\mathrm{L}} = 0.4$ $\quad \sigma^2_{\mathrm{dark}} = 10^{-2}$

Gas: $H_{\mathrm{G}} = 0.9$ $\left| \begin{array}{ll} \sigma^2_{\mathrm{dark}} = 10^{-2} & \text{(dark bubbles)} \\ \sigma^2_{\mathrm{clear}} = 10^{-1} & \text{(clear bubbles)} \end{array} \right.$

High activity: $Q_{\mathrm{G}} = 1200$mL/min - $Q_{\mathrm{L}} = 300$mL/min

Flow	Zooms	Yuan	T-ROF	Free contours	Co-localized contours

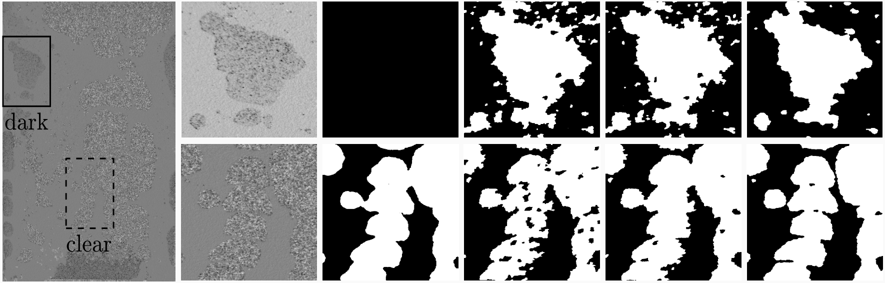

Liquid: $H_{\mathrm{L}} = 0.4$ $\quad \sigma^2_{\mathrm{dark}} = 10^{-2}$

Gas: $H_{\mathrm{G}} = 0.9$ $\quad \left| \begin{array}{ll} \sigma^2_{\mathrm{dark}} = 10^{-2} & \text{(dark bubbles)} \\ \sigma^2_{\mathrm{clear}} = 10^{-1} & \text{(clear bubbles)} \end{array} \right.$

High activity: $Q_{\mathrm{G}} = 1200$mL/min - $Q_{\mathrm{L}} = 300$mL/min

Flow	Zooms	Yuan	T-ROF	Free contours	Co-localized contours

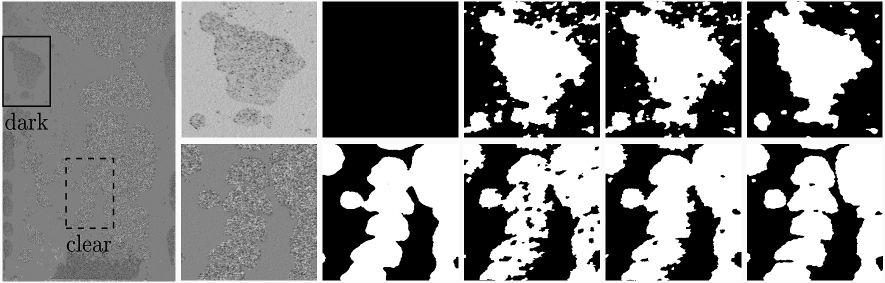

Computational load	Yuan	T-ROF	Free contours	Co-localized contours
	1s	12s	700s	**2100s**

Liquid: $H_{\mathrm{L}} = 0.4$ $\quad \sigma^2_{\mathrm{dark}} = 10^{-2}$

Gas: $H_{\mathrm{G}} = 0.9$ $\quad \sigma^2_{\mathrm{dark}} = 10^{-2}$ (dark bubbles)
$\sigma^2_{\mathrm{clear}} = 10^{-1}$ (clear bubbles)

Regularization parameters selection

$$\left(\widehat{\mathrm{h}}, \widehat{\mathrm{v}}\right)(\mathcal{L}; \Theta) = \underset{\mathrm{h},\mathrm{v}}{\operatorname{argmin}} \sum_{a} \|\log \mathcal{L}_{a,.} - \log(a)\mathrm{h} - \mathrm{v}\|^2 + \theta_1 \mathcal{Q}(\mathrm{Dh}, \mathrm{Dv}; \theta_2)$$

Regularization parameters selection

$$\left(\widehat{\mathrm{h}}, \widehat{\mathrm{v}}\right)(\mathcal{L}; \Theta) = \underset{\mathrm{h},\mathrm{v}}{\operatorname{argmin}} \sum_a \|\log \mathcal{L}_{a,\cdot} - \log(a)\mathrm{h} - \mathrm{v}\|^2 + \theta_1 \mathcal{Q}(\mathrm{Dh}, \mathrm{Dv}; \theta_2)$$

Lin. reg. $\widehat{\mathrm{h}}^{\mathrm{LR}}$

$(\theta_1, \theta_2) = (0, 0)$

Regularization parameters selection

$$\left(\widehat{\mathrm{h}}, \widehat{\mathrm{v}}\right)(\mathcal{L}; \Theta) = \underset{\mathrm{h},\mathrm{v}}{\operatorname{argmin}} \sum_a \|\log \mathcal{L}_{a,\cdot} - \log(a)\mathrm{h} - \mathrm{v}\|^2 + \theta_1 \mathcal{Q}(\mathrm{Dh}, \mathrm{Dv}; \theta_2)$$

Lin. reg. $\widehat{\mathrm{h}}^{\mathrm{LR}}$

Co-localized contours estimate $\widehat{\mathrm{h}}^{\mathrm{C}}$

$(\theta_1, \theta_2) = (0, 0)$

$(\theta_1, \theta_2) = (0.5, 0.5)$

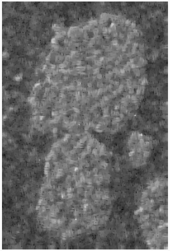

too small

Regularization parameters selection

$$\left(\widehat{\mathrm{h}}, \widehat{\mathrm{v}}\right)(\mathcal{L}; \Theta) = \underset{\mathrm{h},\mathrm{v}}{\operatorname{argmin}} \sum_{a} \|\log \mathcal{L}_{a,\cdot} - \log(a)\mathrm{h} - \mathrm{v}\|^2 + \theta_1 \mathcal{Q}(\mathrm{Dh}, \mathrm{Dv}; \theta_2)$$

Lin. reg. $\widehat{\mathrm{h}}^{\mathrm{LR}}$

Co-localized contours estimate $\widehat{\mathrm{h}}^{\mathrm{C}}$

$(\theta_1, \theta_2) = (0, 0)$

$(\theta_1, \theta_2) = (0.5, 0.5)$

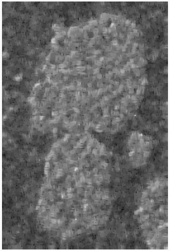

too small

$(\theta_1, \theta_2) = (500, 500)$

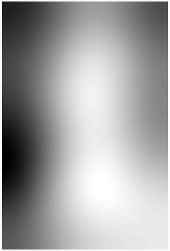

too large

Regularization parameters selection

$$\left(\widehat{\mathrm{h}}, \widehat{\mathrm{v}}\right)(\mathcal{L}; \Theta) = \underset{\mathrm{h},\mathrm{v}}{\operatorname{argmin}} \sum_{a} \|\log \mathcal{L}_{a,\cdot} - \log(a)\mathrm{h} - \mathrm{v}\|^2 + \theta_1 \mathcal{Q}(\mathrm{Dh}, \mathrm{Dv}; \theta_2)$$

Lin. reg. $\widehat{\mathrm{h}}^{\mathrm{LR}}$ | Co-localized contours estimate $\widehat{\mathrm{h}}^{\mathrm{C}}$

$(\theta_1, \theta_2) = (0, 0)$ | $(\theta_1, \theta_2) = (0.5, 0.5)$ | $(\theta_1^\dagger, \theta_2^\dagger) = (11.5, 0.8)$ | $(\theta_1, \theta_2) = (500, 500)$

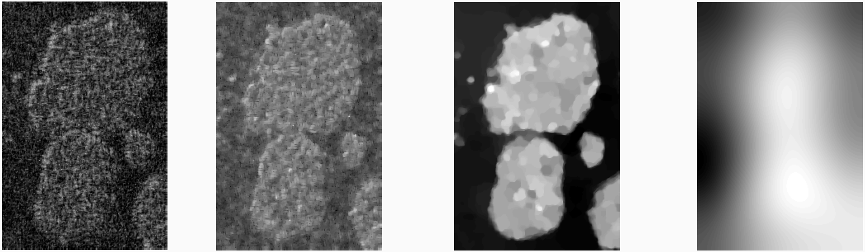

too small | optimal | too large

What *optimal* means? How to determine $\Theta^\dagger = (\theta_1^\dagger, \theta_2^\dagger)$?

Parameter tuning (Grid search)

$$\left(\widehat{\mathrm{h}}, \widehat{\mathrm{v}}\right)(\mathcal{L};\Theta) = \underset{\mathrm{h},\mathrm{v}}{\operatorname{argmin}} \sum_{a} \|\log \mathcal{L}_{a,\cdot} - \log(a)\mathrm{h} - \mathrm{v}\|^2 + \theta_1 \mathcal{Q}(\mathrm{Dh}, \mathrm{Dv}; \theta_2)$$

h: *discriminant*, v: *auxiliary*

Parameter tuning (Grid search)

$$\left(\widehat{\mathrm{h}}, \widehat{\mathrm{v}}\right)(\mathcal{L};\Theta) = \underset{\mathrm{h},\mathrm{v}}{\operatorname{argmin}} \sum_{a} \|\log \mathcal{L}_{a,\cdot} - \log(a)\mathrm{h} - \mathrm{v}\|^2 + \theta_1 \mathcal{Q}(\mathrm{Dh}, \mathrm{Dv}; \theta_2)$$

h: *discriminant*, v: *auxiliary*

$\bar{\mathrm{h}}$: *true* regularity

$$\mathcal{R}(\Theta) = \left\| \widehat{\mathrm{h}}(\mathcal{L};\Theta) - \bar{\mathrm{h}} \right\|^2$$

Parameter tuning (Grid search)

$$\left(\widehat{\mathrm{h}}, \widehat{\mathrm{v}}\right)(\mathcal{L}; \Theta) = \underset{\mathrm{h},\mathrm{v}}{\operatorname{argmin}} \sum_{a} \|\log \mathcal{L}_{a,.} - \log(a)\mathrm{h} - \mathrm{v}\|^2 + \theta_1 \mathcal{Q}(\mathrm{Dh}, \mathrm{Dv}; \theta_2)$$

h: *discriminant*, v: *auxiliary*

$\bar{\mathrm{h}}$: *true* regularity

$$\mathcal{R}(\Theta) = \left\| \widehat{\mathrm{h}}(\mathcal{L}; \Theta) - \bar{\mathrm{h}} \right\|^2$$

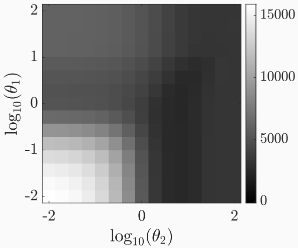

Parameter tuning (Grid search)

$$\left(\widehat{\mathrm{h}}, \widehat{\mathrm{v}}\right)(\mathcal{L};\Theta) = \underset{\mathrm{h},\mathrm{v}}{\operatorname{argmin}} \sum_a \|\log \mathcal{L}_{a,.} - \log(a)\mathrm{h} - \mathrm{v}\|^2 + \theta_1 \mathcal{Q}(\mathrm{Dh}, \mathrm{Dv}; \theta_2)$$

h: *discriminant*, v: *auxiliary*

$\bar{\mathrm{h}}$: *true* regularity

$$\mathcal{R}(\Theta) = \left\|\widehat{\mathrm{h}}(\mathcal{L};\Theta) - \bar{\mathrm{h}}\right\|^2$$

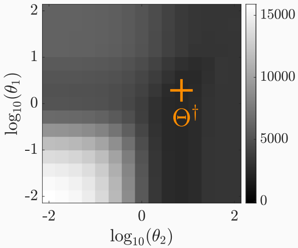

Parameter tuning (Grid search)

$$\left(\widehat{\mathrm{h}}, \widehat{\mathrm{v}}\right)(\mathcal{L}; \Theta) = \underset{\mathrm{h},\mathrm{v}}{\operatorname{argmin}} \sum_{a} \|\log \mathcal{L}_{a,\cdot} - \log(a)\mathrm{h} - \mathrm{v}\|^2 + \theta_1 \mathcal{Q}(\mathrm{Dh}, \mathrm{Dv}; \theta_2)$$

h: *discriminant*, v: *auxiliary*

$\bar{\mathrm{h}}$: *true* regularity

$$\mathcal{R}(\Theta) = \left\| \widehat{\mathrm{h}}(\mathcal{L}; \Theta) - \bar{\mathrm{h}} \right\|^2$$

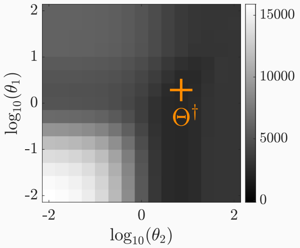

$\bar{\mathrm{h}}$: unknown!

?

Parameter tuning (Grid search)

$$\left(\widehat{\mathrm{h}}, \widehat{\mathrm{v}}\right)(\mathcal{L};\Theta) = \underset{\mathrm{h},\mathrm{v}}{\operatorname{argmin}} \sum_a \|\log \mathcal{L}_{a,\cdot} - \log(a)\mathrm{h} - \mathrm{v}\|^2 + \theta_1 \mathcal{Q}(\mathrm{Dh}, \mathrm{Dv}; \theta_2)$$

h: *discriminant*, v: *auxiliary*

$\bar{\mathrm{h}}$: *true* regularity

$$\mathcal{R}(\Theta) = \left\|\widehat{\mathrm{h}}(\mathcal{L};\Theta) - \bar{\mathrm{h}}\right\|^2$$

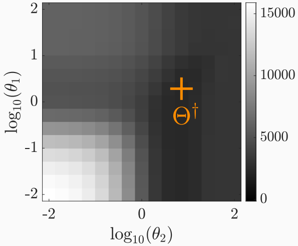

$\bar{\mathrm{h}}$: unknown!

?

Stein Unbiased Risk Estimate

(SURE)

Stein Unbiased Risk Estimate (Principe)

Observations $\mathrm{z} = \bar{\mathrm{x}} + \mathrm{n} \in \mathbb{R}^P$, $\bar{\mathrm{x}}$: truth and $\mathrm{n} \sim \mathcal{N}(0, \kappa^2 \mathrm{I}_P)$

Stein Unbiased Risk Estimate (Principe)

Observations $\mathrm{z} = \bar{\mathrm{x}} + \mathrm{n} \in \mathbb{R}^P$, $\bar{\mathrm{x}}$: truth and $\mathrm{n} \sim \mathcal{N}(0, \kappa^2 \mathrm{I}_P)$

Parametric estimator $(\mathrm{z}; \theta) \mapsto \widehat{\mathrm{x}}(\mathrm{z}; \theta)$

Ex. $$\widehat{\mathrm{x}}(\mathrm{z}; \theta) = \begin{cases} \left(\mathrm{I} + \theta \mathrm{D}^\top \mathrm{D}\right)^{-1} \mathrm{z} & \text{(linear)} \\ \underset{\mathrm{x}}{\operatorname{argmin}} \|\mathrm{z} - \mathrm{x}\|^2 + \theta \mathcal{Q}(\mathrm{D}\mathrm{x}) & \text{(nonlinear)} \end{cases}$$

Stein Unbiased Risk Estimate (Principe)

Observations $\mathrm{z} = \bar{\mathrm{x}} + \mathrm{n} \in \mathbb{R}^P$, $\bar{\mathrm{x}}$: truth and $\mathrm{n} \sim \mathcal{N}(0, \kappa^2 \mathrm{I}_P)$

Parametric estimator $(\mathrm{z}; \theta) \mapsto \widehat{\mathrm{x}}(\mathrm{z}; \theta)$

Ex. $$\widehat{\mathrm{x}}(\mathrm{z}; \theta) = \begin{cases} \left(\mathrm{I} + \theta \mathrm{D}^\top \mathrm{D}\right)^{-1} \mathrm{z} & \text{(linear)} \\ \underset{\mathrm{x}}{\operatorname{argmin}} \|\mathrm{z} - \mathrm{x}\|^2 + \theta \mathcal{Q}(\mathrm{D}\mathrm{x}) & \text{(nonlinear)} \end{cases}$$

Quadratic error $R(\theta) \triangleq \mathbb{E}_{\mathrm{n}} \|\widehat{\mathrm{x}}(\mathrm{z}; \theta) - \bar{\mathrm{x}}\|^2 \overset{?}{=} \mathbb{E}_{\mathrm{n}} \widehat{R}(\mathrm{z}; \theta)$ $\bar{\mathrm{x}}$ unknown

Stein Unbiased Risk Estimate (Principe)

Observations $\mathrm{z} = \bar{\mathrm{x}} + \mathrm{n} \in \mathbb{R}^P$, $\bar{\mathrm{x}}$: truth and $\mathrm{n} \sim \mathcal{N}(0, \kappa^2 \mathrm{I}_P)$

Parametric estimator $(\mathrm{z}; \theta) \mapsto \widehat{\mathrm{x}}(\mathrm{z}; \theta)$

Ex. $\widehat{\mathrm{x}}(\mathrm{z}; \theta) = \begin{cases} \left(\mathrm{I} + \theta \mathrm{D}^\top \mathrm{D}\right)^{-1} \mathrm{z} & \text{(linear)} \\ \underset{\mathrm{x}}{\operatorname{argmin}} \|\mathrm{z} - \mathrm{x}\|^2 + \theta \mathcal{Q}(\mathrm{D}\mathrm{x}) & \text{(nonlinear)} \end{cases}$

Quadratic error $R(\theta) \triangleq \mathbb{E}_{\mathrm{n}} \|\widehat{\mathrm{x}}(\mathrm{z}; \theta) - \bar{\mathrm{x}}\|^2 \overset{?}{=} \mathbb{E}_{\mathrm{n}} \widehat{R}(\mathrm{z}; \theta)$ $\quad$ $\bar{\mathrm{x}}$ unknown

Theorem [C. M. Stein, 1981, *Annals Stat.*]
Let $(\mathrm{z}; \theta) \mapsto \widehat{\mathrm{x}}(\mathrm{z}; \theta)$ an estimator of $\bar{\mathrm{x}}$

- weakly differentiable w.r.t. z,
- such that $\mathrm{n} \mapsto \langle \widehat{\mathrm{x}}(\bar{\mathrm{x}} + \mathrm{n}; \theta), \mathrm{n} \rangle$ is integrable w.r.t. $\mathcal{N}(0, \kappa^2 \mathrm{I}_P)$.

$$\widehat{R}(\mathrm{z}; \theta) \triangleq \|\widehat{\mathrm{x}}(\mathrm{z}; \theta) - \mathrm{z}\|^2 + 2\kappa^2 \operatorname{tr}\left(\partial_{\mathrm{z}} \widehat{\mathrm{x}}(\mathrm{z}; \theta)\right) - \kappa^2 P$$
$$\Longrightarrow R(\theta) = \mathbb{E}_{\mathrm{n}}[\widehat{R}(\mathrm{z}; \theta)].$$

Generalized *Stein Unbiased Risk Estimate*

Observations $\mathrm{z} = \mathrm{A}\bar{\mathrm{x}} + \mathrm{n} \in \mathbb{R}^P, \;\; \bar{\mathrm{x}} \in \mathbb{R}^N$, $\mathrm{A} : \mathbb{R}^{P \times N}$ and $\mathrm{n} \sim \mathcal{N}(0, \mathcal{S})$

E.g. the estimators $\widehat{\mathrm{h}}(\mathcal{L}; \Theta)$ with free or co-localized contours

$\log \mathcal{L} = \mathrm{A}(\bar{\mathrm{h}}, \bar{\mathrm{v}}) + \mathrm{n}$ $\qquad$ $\mathrm{n} \sim \mathcal{N}(0, \mathcal{S})$ $\qquad$ $\mathcal{R} = \|\widehat{\mathrm{h}} - \bar{\mathrm{h}}\|^2$

$\mathrm{A} : (\mathrm{h}, \mathrm{v}) \mapsto \{\log(a)\mathrm{h} + \mathrm{v}\}_a$

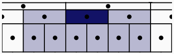

$\Pi : (\mathrm{h}, \mathrm{v}) \mapsto (\mathrm{h}, 0)$

Projected estimation error $\quad R_\Pi(\Theta) \triangleq \mathbb{E}_\mathrm{n} \|\Pi\widehat{\mathrm{x}}(\mathrm{z}; \Theta) - \Pi\bar{\mathrm{x}}\|^2$

Generalized *Stein Unbiased Risk Estimate*

Observations $\mathrm{z} = \mathrm{A}\bar{\mathrm{x}} + \mathrm{n} \in \mathbb{R}^P$, $\bar{\mathrm{x}} \in \mathbb{R}^N$, $\mathrm{A} : \mathbb{R}^{P\times N}$ and $\mathrm{n} \sim \mathcal{N}(0, \mathcal{S})$

E.g. the estimators $\widehat{\mathrm{h}}(\mathcal{L};\Theta)$ with free or co-localized contours

$\log \mathcal{L} = \mathrm{A}(\bar{\mathrm{h}}, \bar{\mathrm{v}}) + \mathrm{n}$ $\qquad$ $\mathrm{n} \sim \mathcal{N}(0, \mathcal{S})$ $\qquad$ $\mathcal{R} = \|\widehat{\mathrm{h}} - \bar{\mathrm{h}}\|^2$

$\mathrm{A} : (\mathrm{h}, \mathrm{v}) \mapsto \{\log(a)\mathrm{h} + \mathrm{v}\}_a$

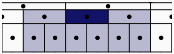

$\Pi : (\mathrm{h}, \mathrm{v}) \mapsto (\mathrm{h}, 0)$

Projected estimation error $\quad R_\Pi(\Theta) \triangleq \mathbb{E}_{\mathrm{n}} \|\Pi\widehat{\mathrm{x}}(\mathrm{z};\Theta) - \Pi\bar{\mathrm{x}}\|^2$

Theorem (B. Pascal et al., 2020, *J. Math. Imaging Vis.*)

Let $(\mathrm{z};\Theta) \mapsto \widehat{\mathrm{x}}(\mathrm{z};\Theta)$ an estimator of $\bar{\mathrm{x}}$

- weakly differentiable w.r.t. z,
- such that $\mathrm{n} \mapsto \langle \Pi\widehat{\mathrm{x}}(\bar{\mathrm{x}} + \mathrm{n};\Theta), \Phi\mathrm{n}\rangle$ is integrable w.r.t. $\mathcal{N}(0, \mathcal{S})$.

$$\widehat{R}(\Theta) \triangleq \|\Phi(\mathrm{A}\widehat{\mathrm{x}}(\mathrm{z};\Theta) - \mathrm{z})\|^2 + 2\mathrm{tr}\left(\mathcal{S}\Phi^\top\Pi\partial_{\mathrm{z}}\widehat{\mathrm{x}}(\mathrm{z};\Theta)\right) - \mathrm{tr}\left(\Phi\mathcal{S}\Phi^\top\right)$$
$$\Longrightarrow R_\Pi(\Theta) = \mathbb{E}_{\mathrm{n}}[\widehat{R}(\Theta)].$$

Computation of the degrees of freedom

Degrees of freedom $\quad \mathrm{dof} \triangleq \mathrm{tr}\left(\mathcal{S}\Phi^\top \Pi \partial_{\mathrm{z}} \widehat{\mathrm{x}}(\mathrm{z};\Theta)\right)$

Computation of the degrees of freedom

Degrees of freedom $\quad \mathrm{dof} \triangleq \mathrm{tr}\left(\mathcal{S}\Phi^\top \Pi \partial_{\mathrm{z}} \widehat{\mathrm{x}}(\mathrm{z};\Theta)\right)$

- **Monte Carlo strategy** (MC) **Large size matrix** $\mathrm{M} \in \mathbb{R}^{P\times P}$

$$\mathrm{tr}(\mathrm{M}) = \mathbb{E}_\varepsilon \left\langle \mathrm{M}\varepsilon, \varepsilon \right\rangle, \quad \varepsilon \sim \mathcal{N}(0, \mathrm{I}_P)$$

Computation of the degrees of freedom

Degrees of freedom $\quad \mathrm{dof} \triangleq \mathrm{tr}\left(\mathcal{S}\Phi^\top \Pi \partial_{\mathrm{z}} \widehat{\mathrm{x}}(\mathrm{z};\Theta)\right)$

- **Monte Carlo strategy** (MC) **Large size matrix** $\mathrm{M} \in \mathbb{R}^{P\times P}$

$$\mathrm{tr}(\mathrm{M}) = \mathbb{E}_\varepsilon \left\langle \mathrm{M}\varepsilon, \varepsilon \right\rangle, \quad \varepsilon \sim \mathcal{N}(0, \mathrm{I}_P)$$

- **Finite Differences** (FD) **Inaccessible Jacobian matrix**

$$\partial_{\mathrm{z}} \widehat{\mathrm{x}}\left[\varepsilon\right] \underset{\nu\to 0}{\simeq} \frac{1}{\nu}\left(\widehat{\mathrm{x}}(\mathrm{z}+\nu\varepsilon;\Theta) - \widehat{\mathrm{x}}(\mathrm{z};\Theta)\right)$$

Computation of the degrees of freedom

Degrees of freedom $\quad \mathrm{dof} \triangleq \mathrm{tr}\left(\mathcal{S}\Phi^\top \Pi \partial_{\mathrm{z}} \widehat{\mathrm{x}}(\mathrm{z};\Theta)\right)$

- **Monte Carlo strategy** (MC) **Large size matrix** $\mathrm{M} \in \mathbb{R}^{P\times P}$

$$\mathrm{tr}(\mathrm{M}) = \mathbb{E}_\varepsilon \left\langle \mathrm{M}\varepsilon, \varepsilon \right\rangle, \quad \varepsilon \sim \mathcal{N}(0, \mathrm{I}_P)$$

- **Finite Differences** (FD) **Inaccessible Jacobian matrix**

$$\partial_{\mathrm{z}} \widehat{\mathrm{x}}\left[\varepsilon\right] \underset{\nu\to 0}{\simeq} \frac{1}{\nu}\left(\widehat{\mathrm{x}}(\mathrm{z}+\nu\varepsilon;\Theta) - \widehat{\mathrm{x}}(\mathrm{z};\Theta)\right)$$

Proposition (B. Pascal et al., 2020, *J. Math. Imaging Vis.*)

Let $(\mathrm{z};\Theta) \mapsto \widehat{\mathrm{x}}(\mathrm{z};\Theta)$ an estimator of $\bar{\mathrm{x}}$

- uniformly Lipschitz continuous w.r.t. z,
- such that $\forall \Theta \in \mathbb{R}^T$, $\widehat{\mathrm{x}}(0_P;\Theta) = 0_N$. Then

$$\mathbb{E}_{\mathrm{n}}\left[\mathrm{dof}\right] = \lim_{\nu\to 0} \mathbb{E}_{\mathrm{n},\varepsilon}\left[\frac{1}{\nu}\left\langle \mathcal{S}\Phi^\top \Pi\left(\widehat{\mathrm{x}}(\mathrm{z}+\nu\varepsilon;\Theta) - \widehat{\mathrm{x}}(\mathrm{z};\Theta)\right), \varepsilon\right\rangle\right]$$

Estimation of the covariance structure of leader coefficients

Log-Gaussianity: $\log \mathcal{L} = \mathrm{A}(\bar{\mathrm{h}}, \bar{\mathrm{v}}) + \mathrm{n}$ with $\mathrm{n} \sim \mathcal{N}(0, \mathcal{S})$

$\Longrightarrow$ Necessary to provide some estimate $\widehat{\mathcal{S}}$ to compute dof and then $\widehat{R}$

Estimation of the covariance structure of leader coefficients

Log-Gaussianity: $\log \mathcal{L} = \mathrm{A}(\bar{\mathrm{h}}, \bar{\mathrm{v}}) + \mathrm{n}$ with $\mathrm{n} \sim \mathcal{N}(0, \mathcal{S})$

$\Longrightarrow$ Necessary to provide some estimate $\widehat{\mathcal{S}}$ to compute dof and then $\widehat{R}$

Covariance structure Noise $\zeta_{j,\underline{n}}$ on $\log \mathcal{L}_{j,\underline{n}}$ at scale 2^j and pixel $\underline{n} = (n_1, n_2)$

$$\mathcal{S}_{j,\underline{n}}^{j',\underline{n}'} \triangleq \mathbb{E}\, \zeta_{j,\underline{n}} \zeta_{j',\underline{n}'} = \mathcal{C}_j^{j'}\, \Xi_j^{j'}(\underline{n} - \underline{n}'), \quad \text{where}\, \mathcal{C}_j^{j'} \triangleq \mathbb{E}\, \zeta_{j,\underline{n}} \zeta_{j',\underline{n}}$$

- $\mathcal{C}_j^{j'}$ independent of $\underline{n}$: inter-scale covariance
- $\Xi_j^{j'}$: stationary spatial correlations, with correlation length $\max(2^j, 2^{j'})$

Estimation of the covariance structure of leader coefficients

Log-Gaussianity: $\log \mathcal{L} = \mathrm{A}(\bar{\mathrm{h}}, \bar{\mathrm{v}}) + \mathrm{n}$ with $\mathrm{n} \sim \mathcal{N}(0, \mathcal{S})$

$\Longrightarrow$ Necessary to provide some estimate $\widehat{\mathcal{S}}$ to compute dof and then $\widehat{R}$

Covariance structure Noise $\zeta_{j,\underline{n}}$ on $\log \mathcal{L}_{j,\underline{n}}$ at scale 2^j and pixel $\underline{n} = (n_1, n_2)$

$$\mathcal{S}_{j,\underline{n}}^{j',\underline{n}'} \triangleq \mathbb{E}\, \zeta_{j,\underline{n}} \zeta_{j',\underline{n}'} = \mathcal{C}_j^{j'}\, \Xi_j^{j'}(\underline{n} - \underline{n}'), \quad \text{where}\, \mathcal{C}_j^{j'} \triangleq \mathbb{E}\, \zeta_{j,\underline{n}} \zeta_{j',\underline{n}}$$

- $\mathcal{C}_j^{j'}$ independent of $\underline{n}$: inter-scale covariance
- $\Xi_j^{j'}$: stationary spatial correlations, with correlation length $\max(2^j, 2^{j'})$

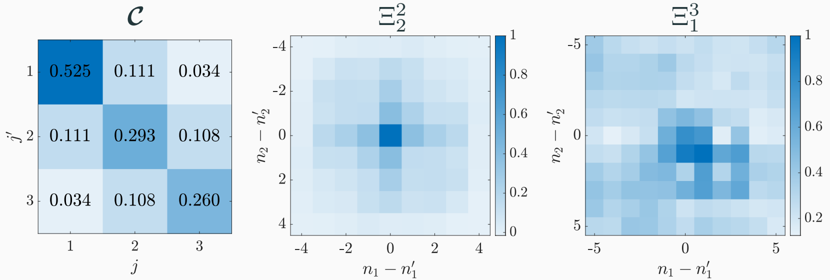

Parameter tuning (Grid search)

$$\left(\widehat{\mathrm{h}}, \widehat{\mathrm{v}}\right)(\mathcal{L};\Theta) = \underset{\mathrm{h},\mathrm{v}}{\operatorname{argmin}} \sum_a \|\log \mathcal{L}_{a,.} - \log(a)\mathrm{h} - \mathrm{v}\|^2 + \theta_1 \mathcal{Q}(\mathrm{Dh}, \mathrm{Dv}; \theta_2)$$

h: *discriminant*, v: *auxiliary*

$\bar{\mathrm{h}}$: *true* regularity

$$\mathcal{R}(\Theta) = \left\|\widehat{\mathrm{h}}(\mathcal{L};\Theta) - \bar{\mathrm{h}}\right\|^2$$

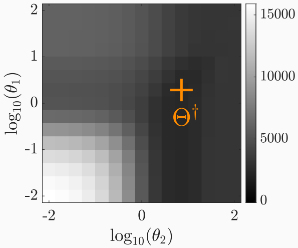

$\bar{\mathrm{h}}$: unknown!

$$\widehat{R}_{\nu,\varepsilon}(\mathcal{L};\Theta|\,\mathcal{S})$$

Parameter tuning (Grid search)

$$\left(\widehat{\mathrm{h}}, \widehat{\mathrm{v}}\right)(\mathcal{L};\Theta) = \underset{\mathrm{h},\mathrm{v}}{\operatorname{argmin}} \sum_{a} \|\log \mathcal{L}_{a,.} - \log(a)\mathrm{h} - \mathrm{v}\|^2 + \theta_1 \mathcal{Q}(\mathrm{Dh}, \mathrm{Dv}; \theta_2)$$

h: *discriminant*, v: *auxiliary*

$\bar{\mathrm{h}}$: *true* regularity

$$\mathcal{R}(\Theta) = \left\| \widehat{\mathrm{h}}(\mathcal{L};\Theta) - \bar{\mathrm{h}} \right\|^2$$

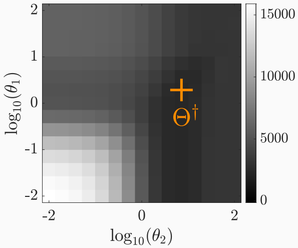

$\bar{\mathrm{h}}$: unknown!

$$\widehat{R}_{\nu,\varepsilon}(\mathcal{L};\Theta|\,\mathcal{S})$$

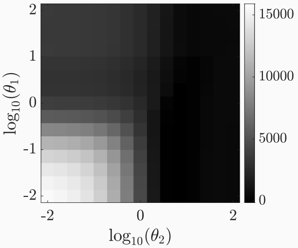

Parameter tuning (Grid search)

$$\left(\widehat{\mathrm{h}}, \widehat{\mathrm{v}}\right)(\mathcal{L}; \Theta) = \underset{\mathrm{h},\mathrm{v}}{\operatorname{argmin}} \sum_{a} \|\log \mathcal{L}_{a,\cdot} - \log(a)\mathrm{h} - \mathrm{v}\|^2 + \theta_1 \mathcal{Q}(\mathrm{Dh}, \mathrm{Dv}; \theta_2)$$

h: *discriminant*, v: *auxiliary*

$\bar{\mathrm{h}}$: *true* regularity

$$\mathcal{R}(\Theta) = \left\|\widehat{\mathrm{h}}(\mathcal{L}; \Theta) - \bar{\mathrm{h}}\right\|^2$$

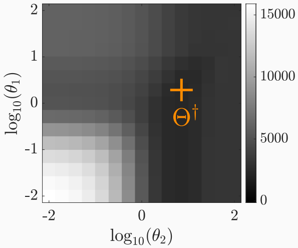

$\bar{\mathrm{h}}$: unknown!

$$\widehat{R}_{\nu,\varepsilon}(\mathcal{L}; \Theta | \mathcal{S})$$

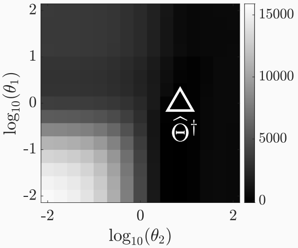

Parameter tuning (Grid search)

$$\left(\widehat{\mathrm{h}}, \widehat{\mathrm{v}}\right)(\mathcal{L};\Theta) = \underset{\mathrm{h},\mathrm{v}}{\operatorname{argmin}} \sum_a \|\log \mathcal{L}_{a,\cdot} - \log(a)\mathrm{h} - \mathrm{v}\|^2 + \theta_1 \mathcal{Q}(\mathrm{Dh}, \mathrm{Dv}; \theta_2)$$

h: *discriminant*, v: *auxiliary*

$\bar{\mathrm{h}}$: *true* regularity

$$\mathcal{R}(\Theta) = \left\|\widehat{\mathrm{h}}(\mathcal{L};\Theta) - \bar{\mathrm{h}}\right\|^2$$

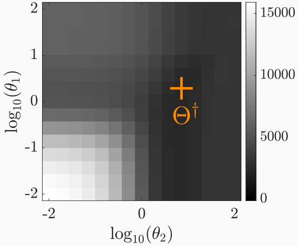

$\bar{\mathrm{h}}$: unknown!

$$\widehat{R}_{\nu,\varepsilon}(\mathcal{L};\Theta|\,\mathcal{S})$$

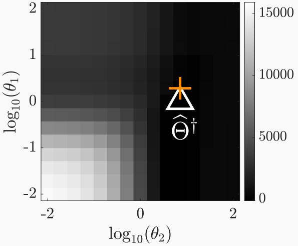

Parameter tuning (Automatic selection)

$$\left(\widehat{\mathrm{h}}, \widehat{\mathrm{v}}\right)(\mathcal{L};\Theta) = \underset{\mathrm{h},\mathrm{v}}{\operatorname{argmin}} \sum_a \|\log \mathcal{L}_{a,.} - \log(a)\mathrm{h} - \mathrm{v}\|^2 + \theta_1 \mathcal{Q}(\mathrm{Dh}, \mathrm{Dv}; \theta_2)$$

h: *discriminant*, v: *auxiliary*

$\bar{\mathrm{h}}$: *true* regularity

$$\mathcal{R}(\Theta) = \left\|\widehat{\mathrm{h}}(\mathcal{L};\Theta) - \bar{\mathrm{h}}\right\|^2$$

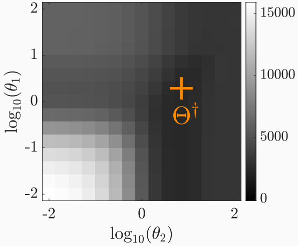

$\bar{\mathrm{h}}$: unknown!

$$\widehat{R}_{\nu,\varepsilon}(\mathcal{L};\Theta|\,\mathcal{S})$$

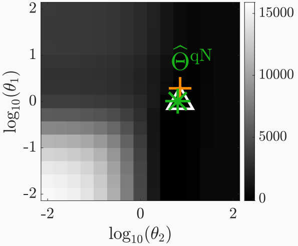

Parameter tuning (Automatic selection)

$$\left(\widehat{\mathrm{h}}, \widehat{\mathrm{v}}\right)(\mathcal{L};\Theta) = \underset{\mathrm{h},\mathrm{v}}{\operatorname{argmin}} \sum_{a} \|\log \mathcal{L}_{a,\cdot} - \log(a)\mathrm{h} - \mathrm{v}\|^2 + \theta_1 \mathcal{Q}(\mathrm{Dh}, \mathrm{Dv}; \theta_2)$$

h: *discriminant*, v: *auxiliary*

$\bar{\mathrm{h}}$: *true* regularity

$$\mathcal{R}(\Theta) = \left\| \widehat{\mathrm{h}}(\mathcal{L};\Theta) - \bar{\mathrm{h}} \right\|^2$$

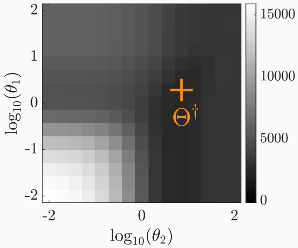

$\bar{\mathrm{h}}$: unknown!

$$\widehat{R}_{\nu,\varepsilon}(\mathcal{L};\Theta|\,\mathcal{S})$$

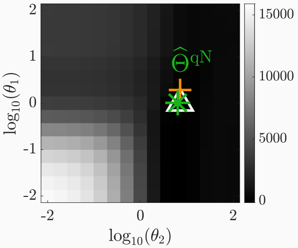

Automated selection of regularization parameters

$$\left(\widehat{\mathrm{h}}, \widehat{\mathrm{v}}\right)(\mathcal{L};\Theta) = \underset{\mathrm{h},\mathrm{v}}{\operatorname{argmin}} \sum_{a} \|\log \mathcal{L}_{a,\cdot} - \log(a)\mathrm{h} - \mathrm{v}\|^2 + \theta_1 \mathcal{Q}(\mathrm{Dh}, \mathrm{Dv}; \theta_2)$$

Example	$\widehat{\mathrm{h}}^{\mathsf{F}}(\mathcal{L};\Theta^{\dagger})$ (grid)	$\widehat{\mathrm{h}}^{\mathsf{F}}(\mathcal{L};\widehat{\Theta}^{\dagger})$ (grid)	$\widehat{\mathrm{h}}^{\mathsf{F}}(\mathcal{L};\widehat{\Theta}^{\mathsf{qN}})$ (quasi-Newton)

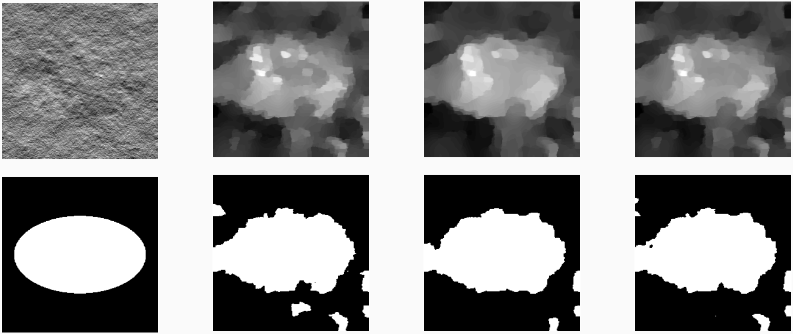

225 calls of the estimator over the grid v.s. **40** for quasi-Newton

Isotropic texture segmentation: take home messages

- **Fractal texture model based on local *regularity* and *variance***
  - appropriate for real-world texture characterization
  - complementary attributes able to finely discriminate

Isotropic texture segmentation: take home messages

- **Fractal texture model based on local *regularity* and *variance***
  - appropriate for real-world texture characterization
  - complementary attributes able to finely discriminate
- **Simultaneous estimation and regularization**
  - significant decrease of the estimation error
  - accurate and regular *co-localized* contours

Isotropic texture segmentation: take home messages

- **Fractal texture model based on local *regularity* and *variance***
  - appropriate for real-world texture characterization
  - complementary attributes able to finely discriminate
- **Simultaneous estimation and regularization**
  - significant decrease of the estimation error
  - accurate and regular *co-localized* contours
- **Fast algorithms for automated tuning of hyperparameters**
  - possibility to manage huge amount of data
  - amenable to process data corrupted by *correlated* noise
  - ensured objectivity and reproducibility

GSUGAR: Matlab toolbox for texture segmentation

Mask

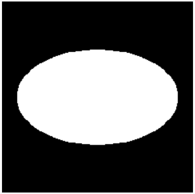

Texture

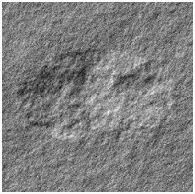

$\widehat{h}^{\mathrm{LR}}$

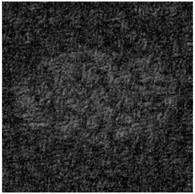

$\widehat{h}^{\mathrm{ROF}}$

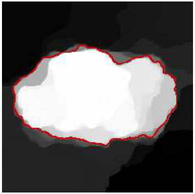

$\widehat{h}^{\mathrm{J}}$

$\widehat{h}^{\mathrm{C}}$

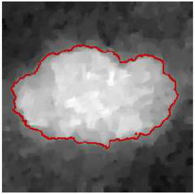

github.com/bpascal-fr/gsugar: demo_gsugar_2D

GSUGAR: Changepoint detection in monofractal signals

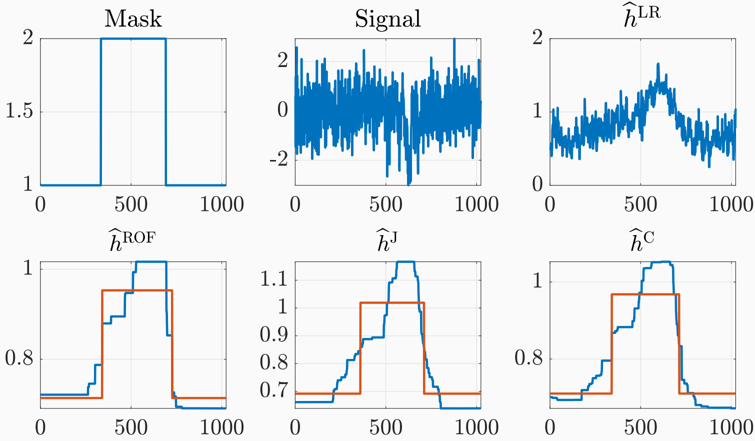

github.com/bpascal-fr/gsugar: demo_gsugar_1D

Anisotropic textures analysis

Anisotropic fractal textures in real data

Breast cancer:

- most common cancer amongst women with ~ 1 over 8 diagnosed
- early detection is critical for the patient's survival

Anisotropic fractal textures in real data

Breast cancer:

- most common cancer amongst women with ~ 1 over 8 diagnosed
- early detection is critical for the patient's survival

X-ray imaging: most used imaging technique yielding a so-called *mammogram*

Anisotropic fractal textures in real data

Breast cancer:

- most common cancer amongst women with $\sim$ 1 over 8 diagnosed
- early detection is critical for the patient's survival

X-ray imaging: most used imaging technique yielding a so-called *mammogram*

Assessment by a radiologist:

- fatty tissues: translucent to X-rays (black)
- epithelial & stromal tissues: absorb X-rays (white)
- tumorous tissues: **also absorb X-rays** (white)

$\Longrightarrow$ errors of both I and II types in anomaly detection

Anisotropic fractal textures in real data

Breast cancer:

- most common cancer amongst women with $\sim$ 1 over 8 diagnosed
- early detection is critical for the patient's survival

X-ray imaging: most used imaging technique yielding a so-called *mammogram*

Assessment by a radiologist:

- fatty tissues: translucent to X-rays (black)
- epithelial & stromal tissues: absorb X-rays (white)
- tumorous tissues: **also absorb X-rays** (white)

$\Longrightarrow$ errors of both I and II types in anomaly detection

Computer-Aided Detection: used in 92% of screening mammograms in U.S.

Anisotropic fractal textures in real data

Self-similar textures:

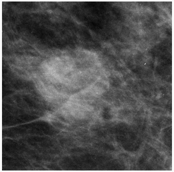

Mammogram

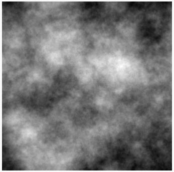

fractional Brownian field

Anisotropic fractal textures in real data

Self-similar textures:

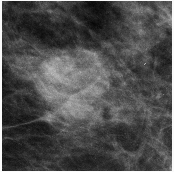

Mammogram

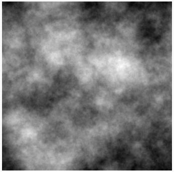

fractional Brownian field

Isotropic fractal analysis, e.g., fractal dimension of a rough surface, for

- classification of mammogram density [Caldwell et al., 1990, *Phys. Med. Biol.*]
- lesion detection in mammograms [Burgess et al., 2001, *Med. Biol.*]
- assessment of breast cancer risk [Heine et al., 2002, *Acad. Radiol.*]

Anisotropic fractal textures in real data

Self-similar textures:

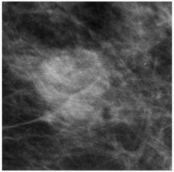

Mammogram

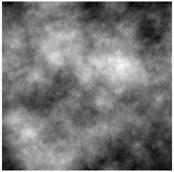

fractional Brownian field

Isotropic fractal analysis, e.g., fractal dimension of a rough surface, for

- classification of mammogram density [Caldwell et al., 1990, *Phys. Med. Biol.*]
- lesion detection in mammograms [Burgess et al., 2001, *Med. Biol.*]
- assessment of breast cancer risk [Heine et al., 2002, *Acad. Radiol.*]

Anisotropy in mammograms

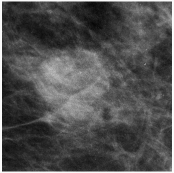

mass

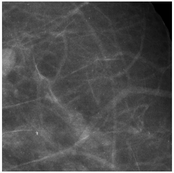

tissues

[F. J. Richard et al., 2010, *J. Math. Imaging Vis.*; F. J. Richard, 2016, *Spat. Stat.*]

Anisotropic Self-Similar Fields

Definition: Let $f \in L^1(\min(1, |\underline{\xi}|^2)\mathrm{d}\xi)$ a **spectral density**. The associated *Bonami-Estrade field* X^f is defined through its harmonizable representation:

$$\mathsf{X}^f : \begin{cases} \mathbb{R}^2 & \to & \mathbb{R} \\ \underline{x} & \mapsto & \displaystyle\int_{\mathbb{R}^2} \left(\exp(\mathrm{i}\underline{x} \cdot \underline{\xi}) - 1\right) \sqrt{f(\underline{\xi})}\widetilde{\mathsf{W}}(\mathrm{d}\xi) \end{cases}$$

with W a Brownian measure; $\widetilde{\mathsf{W}}$ its Fourier transform.

[A. Bonami & A. Estrade, 2003, *J. Fourier Anal. Appl.*]

Anisotropic Self-Similar Fields

Definition: Let $f \in L^1(\min(1, |\underline{\xi}|^2)\mathrm{d}\xi)$ a **spectral density**. The associated *Bonami-Estrade field* X^f is defined through its harmonizable representation:

$$\mathsf{X}^f : \begin{cases} \mathbb{R}^2 & \to & \mathbb{R} \\ \underline{x} & \mapsto & \displaystyle\int_{\mathbb{R}^2} \left(\exp(\mathrm{i}\underline{x} \cdot \underline{\xi}) - 1\right) \sqrt{f(\underline{\xi})}\widetilde{\mathsf{W}}(\mathrm{d}\xi) \end{cases}$$

with W a Brownian measure; $\widetilde{\mathsf{W}}$ its Fourier transform.

[A. Bonami & A. Estrade, 2003, *J. Fourier Anal. Appl.*]

Spectral density encodes visual and statistical properties such as

- (an)isotropy
- preferential directions
- short or long range dependencies

[H. Biermé, 2019, *Lecture Notes in Mathematics, Springer*]

The Anisotropic Fractional Brownian Field

The **anisotropic fractional Brownian field** is defined as

$$\mathsf{X}^f(\underline{x}) = \int_{\mathbb{R}^2} \left(\exp(\mathrm{i}\underline{x}\cdot\underline{\xi}) - 1\right) \sqrt{f(\underline{\xi})}\widetilde{\mathsf{W}}(\mathrm{d}\xi)$$

with **spectral density** $f(\underline{\xi}) = \tau\left(\frac{\underline{\xi}}{\|\underline{\xi}\|}\right)\|\underline{\xi}\|^{-2h\left(\frac{\underline{\xi}}{\|\underline{\xi}\|}\right)-2}$ with

- $\tau : \mathbb{S}_1 \to \mathbb{R}_+$ the **topothesy** function
- $h : \mathbb{S}_1 \to]0,1[$ the **Hurst** function

Package PyAFBF for the simulation of rough anisotropic image textures
fjprichard.github.io/PyAFBF

[F. J. Richard & H. Biermé, 2011, *J. Math. Imaging Vis.*]

Particular (anisotropic) fractional Brownian fields

H-fractional Brownian field H-fBf: $h \equiv H$, $\tau \equiv \sigma^2/\mathcal{C}_H$ both **constant**

Field X^f

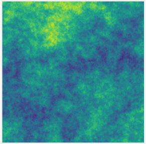

Hurst function h

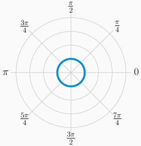

Topothesy function τ

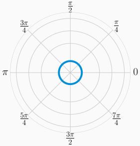

[L. Davy et al., 2025, *Preprint*]

H-fractional Brownian field H-fBf: $h \equiv H$, $\tau \equiv \sigma^2 / \mathcal{C}_H$ both **constant**

Field X^f

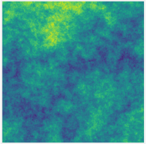

Hurst function h

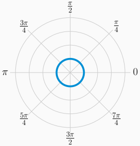

Topothesy function τ

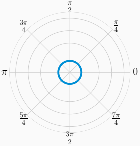

H-anisotropic fractional Brownian field H-afBf: $h \equiv H$ **constant**

$\Longrightarrow$ directional modulation of the variance of the field via τ

Field X^f

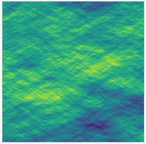

Hurst function h

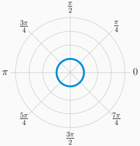

Topothesy function τ

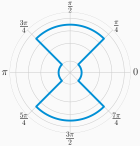

[L. Davy et al., 2025, *Preprint*]

General anisotropic fractional Brownian fields

Anisotropic fractional Brownian field afBf: modulation of both

$\Longrightarrow$ the variance of the field via τ

$\Longrightarrow$ the decay the spectral density via h

X^f

$h(\vartheta)$

$\tau(\vartheta)$

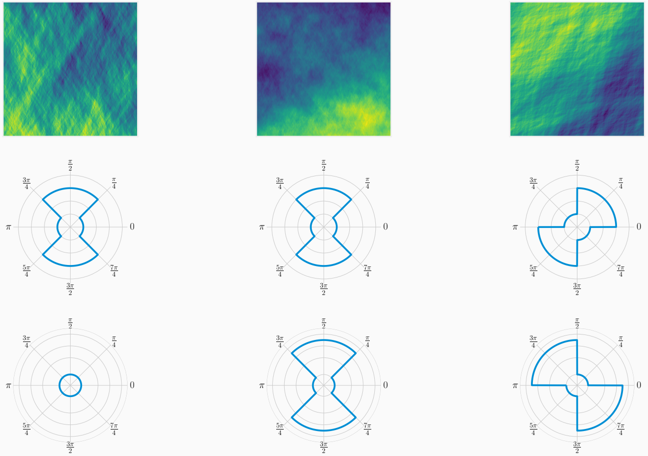

fjprichard.github.io/PyAFBF [L. Davy et al., 2025, *Preprint*]

Uniform Hölder regularity of anisotropic fields

Definition: The uniform Hölder regularity of the field X^f is $H_{\min}$ if

$$\exists A, B > 0, \quad \text{such that: } \forall \|\underline{\xi}\| > A, \quad f(\underline{\xi}) \leq B \|\underline{\xi}\|^{-2H_{\min}-2}.$$

Anisotropic fractional Brownian fields have uniform Hölder regularity

$$H_{\min} = \operatorname*{essinf}_{\vartheta \in \mathbb{S}_1} h(\vartheta)$$

From **Kolmogorov-Chensov theorem**

- H-(isotropic) fractional Brownian field B_H: $H_{\min} = H$
- H-anisotropic fractional Brownian field B_H: $H_{\min} = H$

Same uniform Hölder regularity $H_{\min}$ for H-fBf and H-afBf.

[S. Cohen & J. Istas, 2013, *Springer*]

Analysis of anisotropic fractal textures

- **Directional increments & Radon transform**: [H. Biermé et al., 2008, *ESAIM: Proba. Stat.*]

$$(\forall(\vartheta,t)\in\mathbb{S}^1\times\mathbb{R})\quad \mathcal{R}_\rho \mathsf{X}(\vartheta,t)=\int_{\mathbb{R}} \mathsf{X}(s\vartheta^\perp+t\vartheta)\rho(s)\,\mathrm{d}s$$

windowed Radon transform with ρ Schwartz class

Analysis of anisotropic fractal textures

- **Directional increments & Radon transform**: [H. Biermé et al., 2008, *ESAIM: Proba. Stat.*]

$$(\forall(\vartheta, t) \in \mathbb{S}^1 \times \mathbb{R}) \quad \mathcal{R}_\rho \mathsf{X}(\vartheta, t) = \int_{\mathbb{R}} \mathsf{X}(s\vartheta^\perp + t\vartheta)\rho(s)\,\mathrm{d}s$$

windowed Radon transform with ρ Schwartz class

- **X-let and scattering transform**: [S. Mallat, 2008, *Acad. Press*; J. Bruna, 2013, *PhD thesis*] kymat.io

scattering coefficients of order n: $\quad |||\mathsf{X} * \psi_{\theta_1,j_1}| * \psi_{\theta_2,j_2}| \ldots * \psi_{\theta_n,j_n}| * \varphi_J$

Analysis of anisotropic fractal textures

- **Directional increments & Radon transform**: [H. Biermé et al., 2008, *ESAIM: Proba. Stat.*]

$$(\forall(\vartheta,t)\in\mathbb{S}^1\times\mathbb{R})\quad \mathcal{R}_\rho\mathsf{X}(\vartheta,t)=\int_{\mathbb{R}}\mathsf{X}(s\vartheta^\perp+t\vartheta)\rho(s)\,\mathrm{d}s$$

windowed Radon transform with ρ Schwartz class

- **X-let and scattering transform**: [S. Mallat, 2008, *Acad. Press*; J. Bruna, 2013, *PhD thesis*] kymat.io

scattering coefficients of order n: $\quad |||\mathsf{X}*\psi_{\theta_1,j_1}|*\psi_{\theta_2,j_2}|\ldots*\psi_{\theta_n,j_n}|*\varphi_J$

- **Monogenic Images** [H. Biermé et al., 2024,*Preprint*]

$$\mathcal{M}\mathsf{X}(\mathsf{w})=(\langle\mathsf{X},\mathsf{w}\rangle,\langle\mathcal{R}_1\mathsf{X},\mathsf{w}\rangle,\langle\mathcal{R}_2\mathsf{X},\mathsf{w}\rangle)$$

$\mathcal{R}_k\mathsf{w}(\underline{x})=\dfrac{1}{2\pi}\lim\limits_{\varepsilon\to 0}\displaystyle\int_{\mathbb{R}^2\setminus\mathrm{B}(0,\varepsilon)}\frac{x_k-y_k}{\|\underline{x}-\underline{y}\|^3}\mathsf{w}(\underline{y})\,d\underline{y}$ Riesz transform

Wavelet analysis of anisotropic fractal textures

Multiband complex wavelet transform

$\left(\psi^{(1)},\dots,\psi^{(B)}\right)$ B complex mother wavelets: $\psi^{(b)}:\mathbb{R}^2\to\mathbb{C}$ such that

$$\psi^{(b)}=\psi^{(0)}\left(\mathcal{R}_{\vartheta_b}^{\top}\cdot\right)\quad \widetilde{\psi}^{(b)}=\widetilde{\psi}^{(0)}\left(\mathcal{R}_{\vartheta_b}^{\top}\cdot\right)$$

for $\psi^{(0)}$ a frequency-direction selective complex mother wavelet;

multiband wavelet coefficients: $\zeta_{j,\underline{k}}^{(b)}=\langle \mathsf{X},\psi_{j,\underline{k}}^{(b)}\rangle$

Field X^f

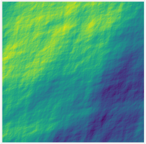

Hurst function h

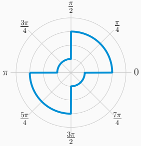

Topothesy function τ

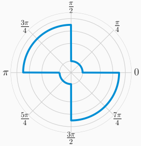

[L. Davy et al., 2025, *Preprint*]

Segmentation of piecewise homogeneous anisotropic textures

Synthesis M**-class piecewise homogeneous Gaussian Bonami-Estrade field**

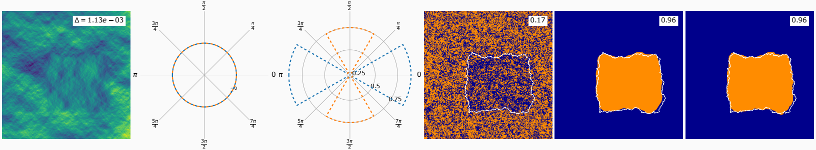

- $M = 2$ textures: background vs. central rectangle
- **same** topothesy
- **different** Hurst functions

[L. Davy et al., 2025, *Preprint*]

Synthesis M**-class piecewise homogeneous Gaussian Bonami-Estrade field**

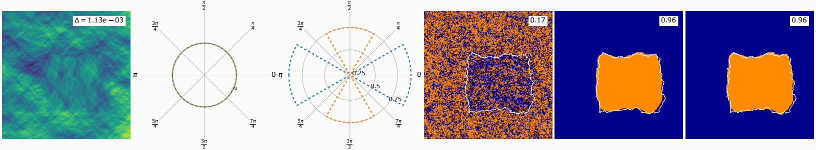

- $M = 2$ textures: background vs. central rectangle
- **same** topothesy
- **different** Hurst functions

Segmentation: requires accurate contour localization

Non-decimated Dual Tree Complex Wavelet Transform $\zeta^{(b)}_{j,\underline{n}}$

Theorem Let X^f a piecewise homogeneous Gaussian Bonami-Estrade field.
The multiband wavelet coefficients $\zeta^{(b)}_{j,\underline{n}} = \langle \mathsf{X}^f, \psi^{(b)}_{j,\underline{n}} \rangle$ satisfy

$$\zeta^{(b)}_{j,\underline{n}} \sim \mathcal{N}\left(0, \left(\sigma^{(b)}_{j,\underline{n}}\right)^2\right) \quad \text{with} \quad \left(\sigma^{(b)}_{j,\underline{n}}\right)^2 \sim \mathcal{V}(\tau, h, \psi^{(b)}) 2^{j2H\left(h,\psi^{(b)}\right)}$$

[L. Davy et al., 2025, *Preprint*]

Anisotropic texture segmentation: take home messages

- **Non-decimated multiband wavelet coefficients**
  - behaves locally approximately as **power laws**
  - local scaling exponents depending on **Hurst function**
  - local intercept providing information about **topothesy function**

Anisotropic texture segmentation: take home messages

- **Non-decimated multiband wavelet coefficients**
  - behaves locally approximately as **power laws**
  - local scaling exponents depending on **Hurst function**
  - local intercept providing information about **topothesy function**
- **Regularized estimates of scaling exponents and intercept**
  - approximate **power-law** model for multiband wavelet coefficients
  - penalization enforcing pixel-wise spatial **piecewise constancy**
  - excellent segmentation performance in **various configurations**

Natural textures characterized by joint fractal and anisotropy properties

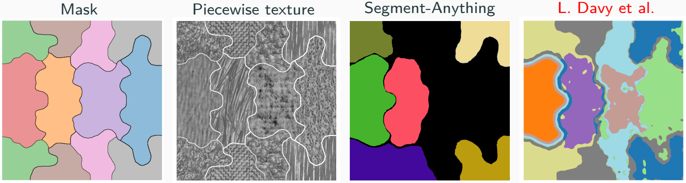

[L. Davy et al., 2023, *ICASSP*; L. Davy et al., 2024, *EUSIPCO*; L. Davy et al., 2025, *Preprint*]